

A journey in particle physics:

From precision measurement of the heaviest particle to new physics search with the lightest (charged) particles

Costas Vellidis

Fermilab

University of Pisa seminar, July 21, 2016

Outline

Top quark mass measurement at CDF

- Top mass status
- This measurement
- Method
- Prospects
- Summary

Outline

Top quark mass measurement at CDF

- Top mass status
- This measurement
- Method
- Prospects
- Summary

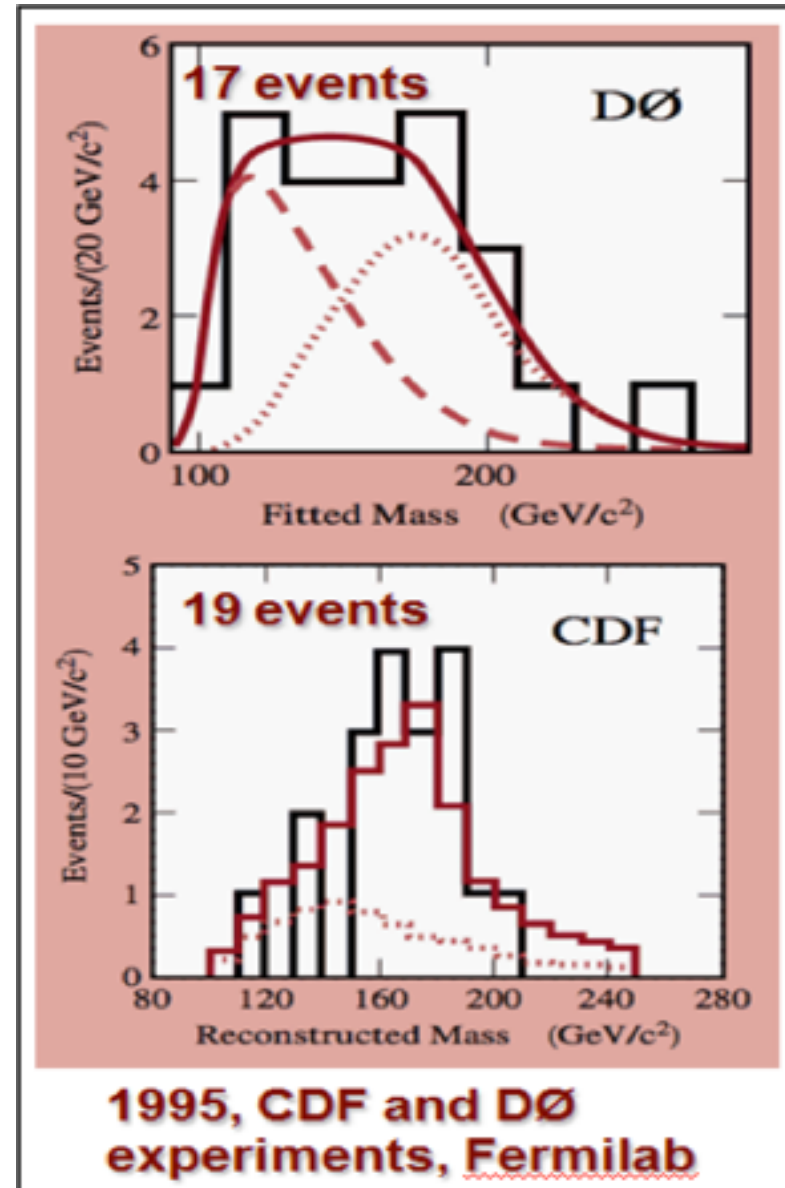
Search for neutrinoless muon-to-electron conversion

- Motivation
- Experimental technique
- Magnetic field studies
- Summary

Top mass measurement in the semileptonic
decay channel using the full CDF sample

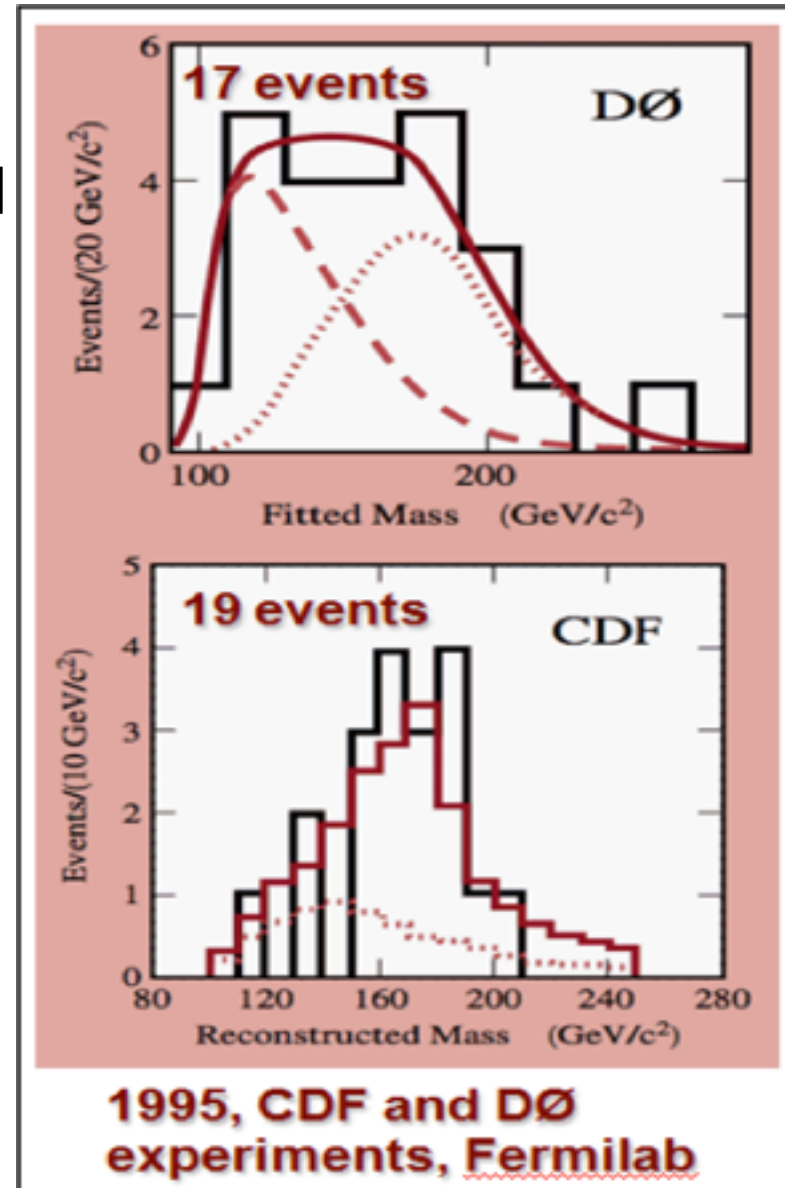
Basic facts about top

✓ Discovered at the Tevatron in 1995



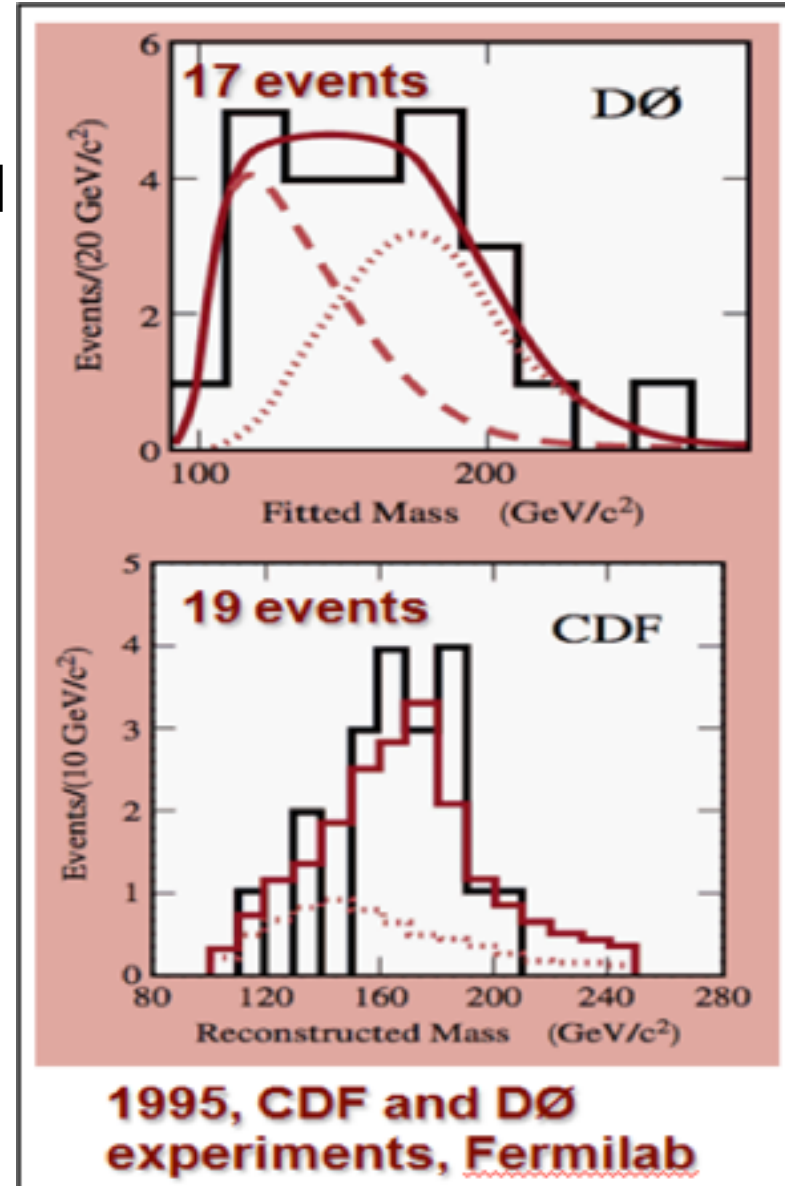
Basic facts about top

- ✓ Discovered at the Tevatron in 1995
- ✓ Heaviest known particle, sets a hard scale



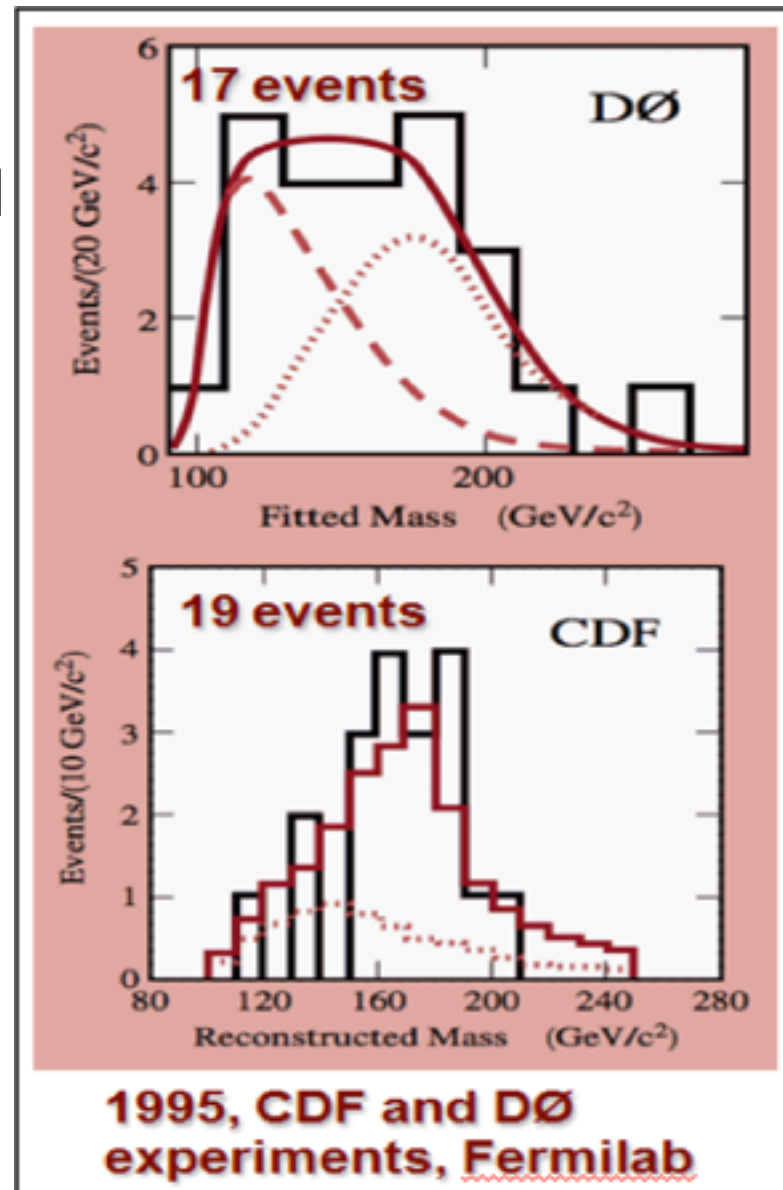
Basic facts about top

- ✓ Discovered at the Tevatron in 1995
- ✓ Heaviest known particle, sets a hard scale
- ✓ $\Gamma = 2.0 \pm 0.5 \text{ GeV}$ (or $\tau = 3 \times 10^{-25} \text{ s}$)
→ lifetime shorter than hadronization time scale



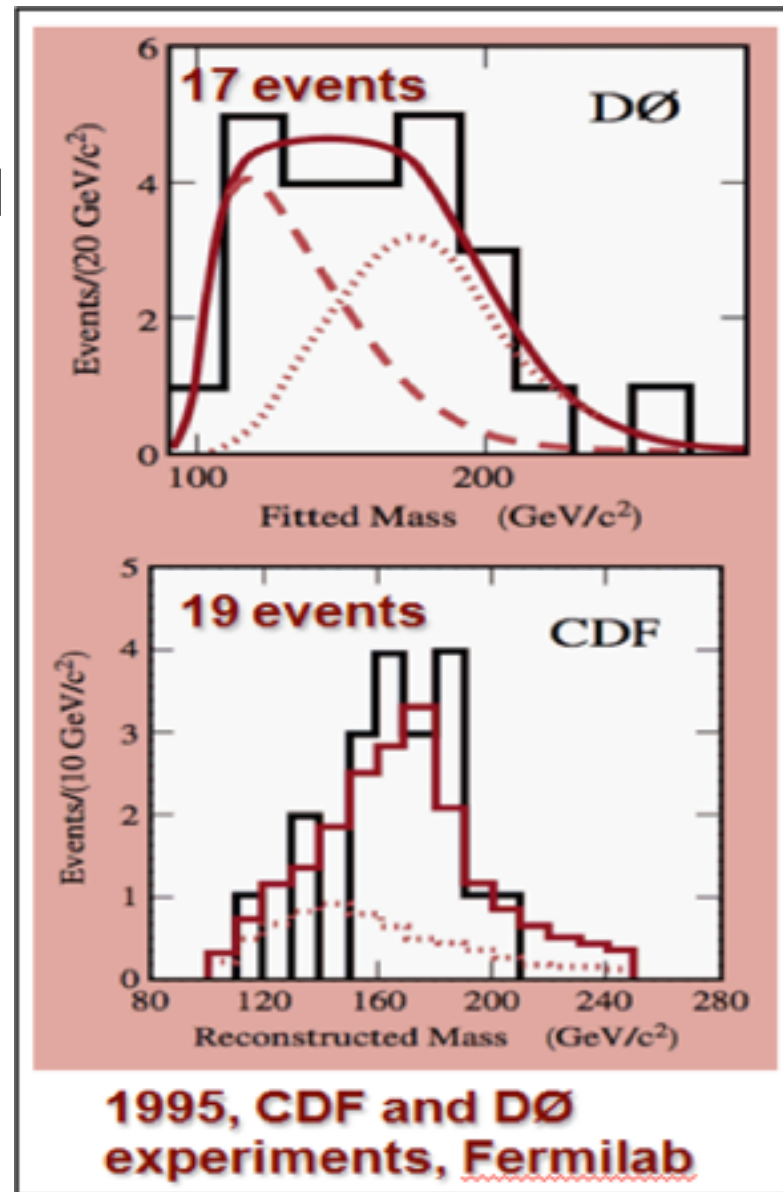
Basic facts about top

- ✓ Discovered at the Tevatron in 1995
- ✓ Heaviest known particle, sets a hard scale
- ✓ $\Gamma = 2.0 \pm 0.5 \text{ GeV}$ (or $\tau = 3 \times 10^{-25} \text{ s}$)
→ lifetime shorter than hadronization time scale
- ✓ Top physics (mainly) described by pQCD



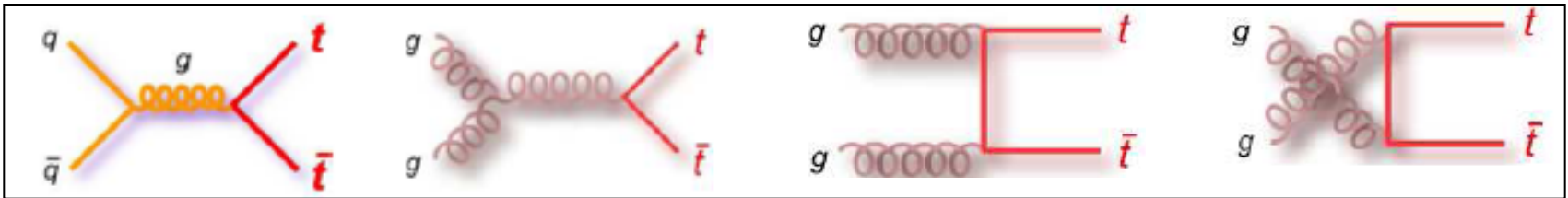
Basic facts about top

- ✓ Discovered at the Tevatron in 1995
- ✓ Heaviest known particle, sets a hard scale
- ✓ $\Gamma = 2.0 \pm 0.5 \text{ GeV}$ (or $\tau = 3 \times 10^{-25} \text{ s}$)
→ lifetime shorter than hadronization time scale
- ✓ Top physics (mainly) described by pQCD
- ✓ But top is colored and unstable particle: non-perturbative effects enter through the back door



Top pair production and decay

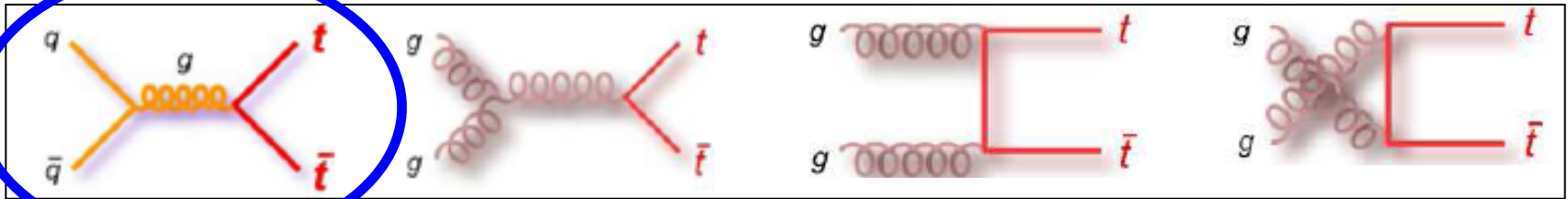
Produced mainly through the strong interaction:
 $\sigma \sim 7 \text{ pb}$ (Tevatron)



Top pair production and decay

Produced mainly through the strong interaction:

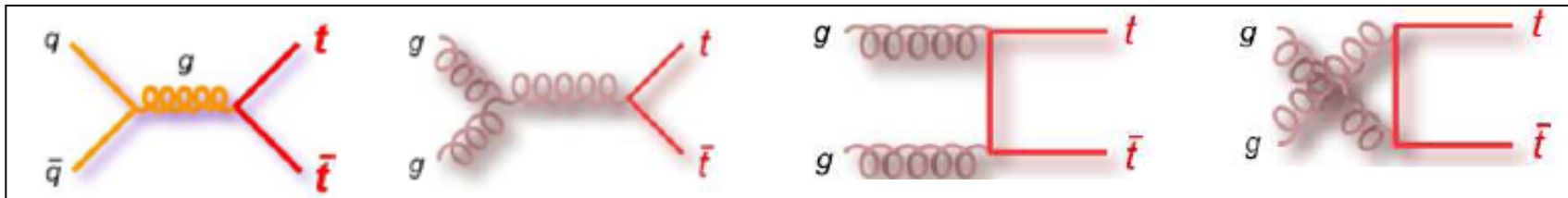
$\sigma \sim 7 \text{ pb}$ (Tevatron)



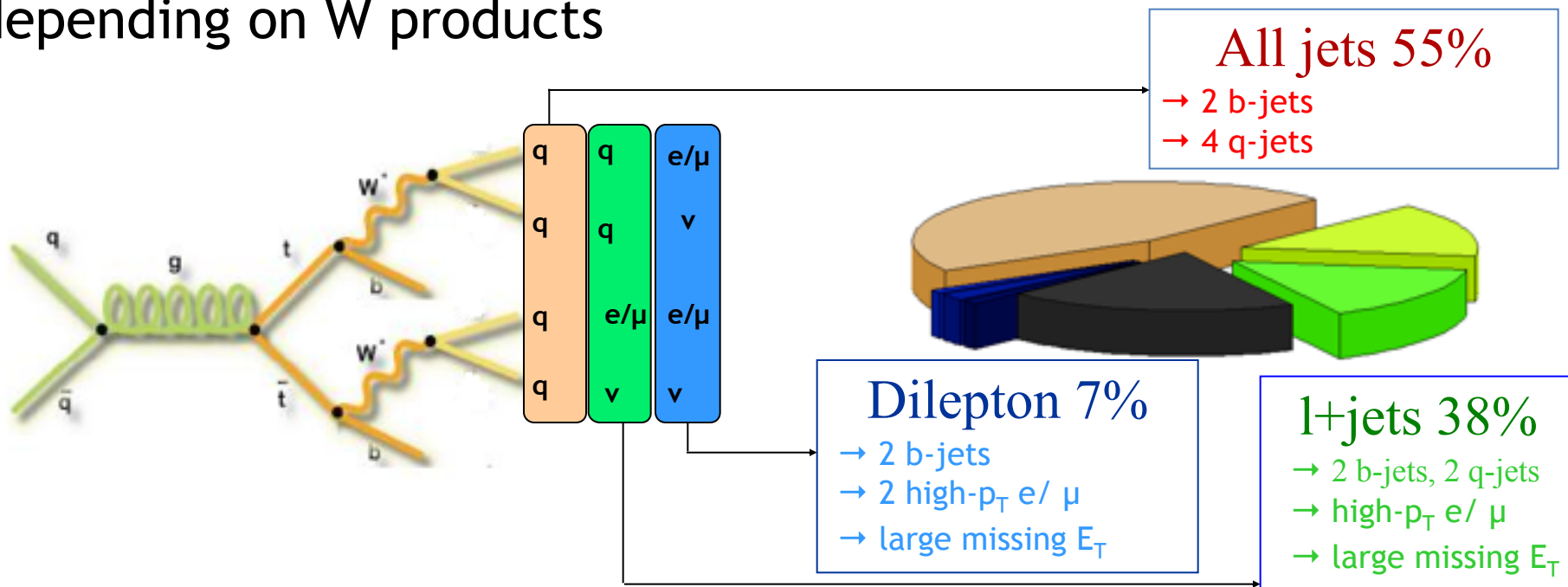
~85% at the Tevatron

Top pair production and decay

Produced mainly through the strong interaction:
 $\sigma \sim 7 \text{ pb}$ (Tevatron)



Decaying in $Wb \sim 100\%$ \rightarrow 3 possible signatures depending on W products

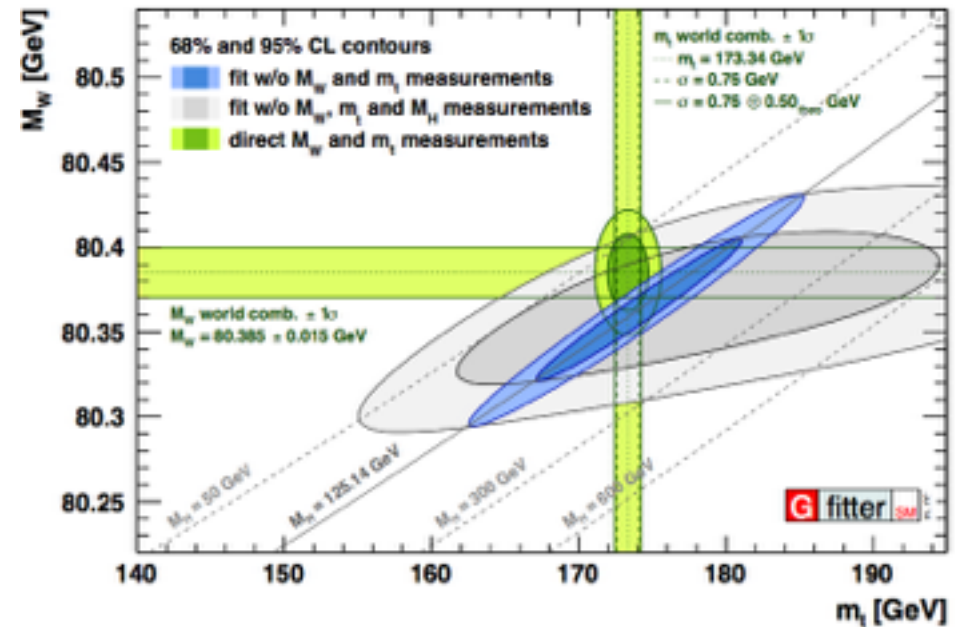


Why care about top mass precision?

- ✓ The only top property not predicted by theory

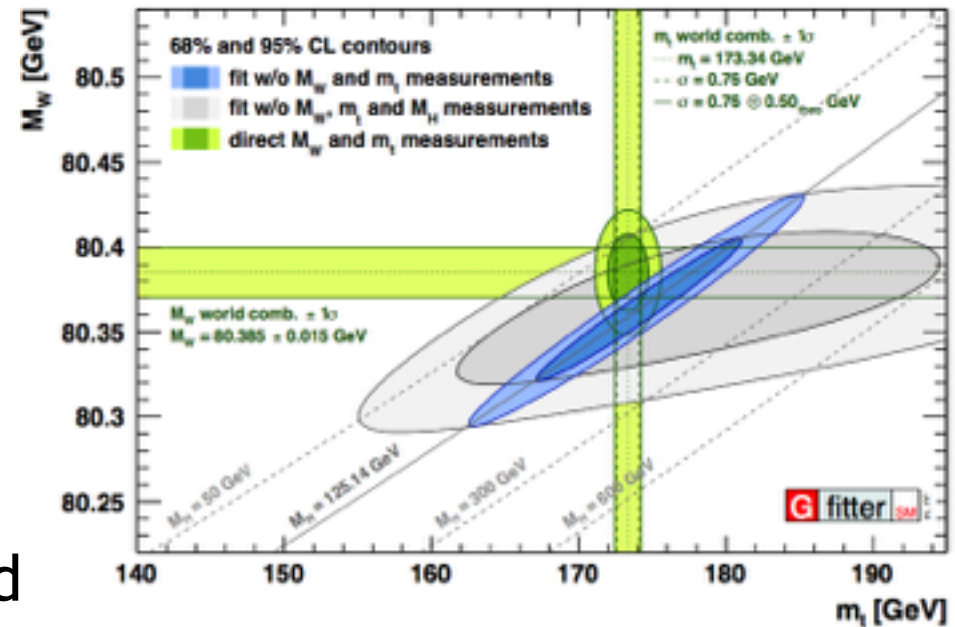
Why care about top mass precision?

- ✓ The only top property not predicted by theory
- ✓ Close to electroweak symmetry breaking scale → impact on precision Higgs physics



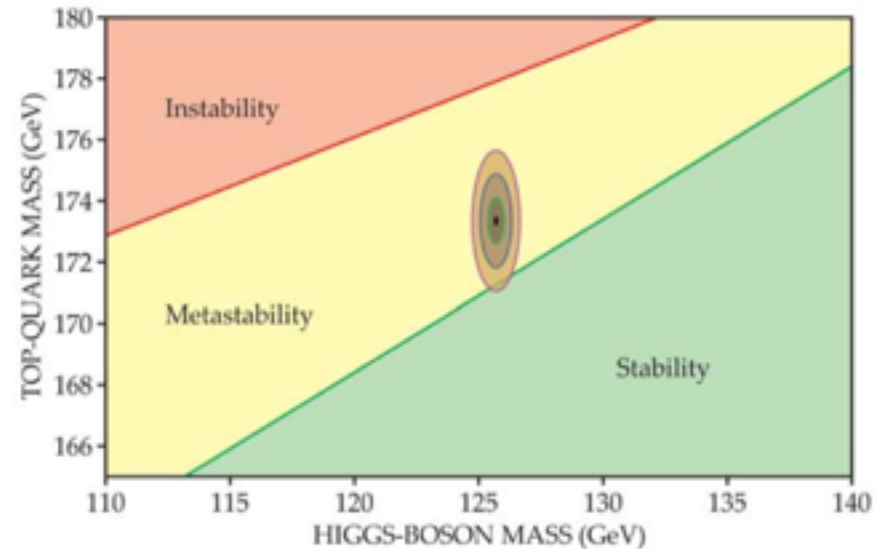
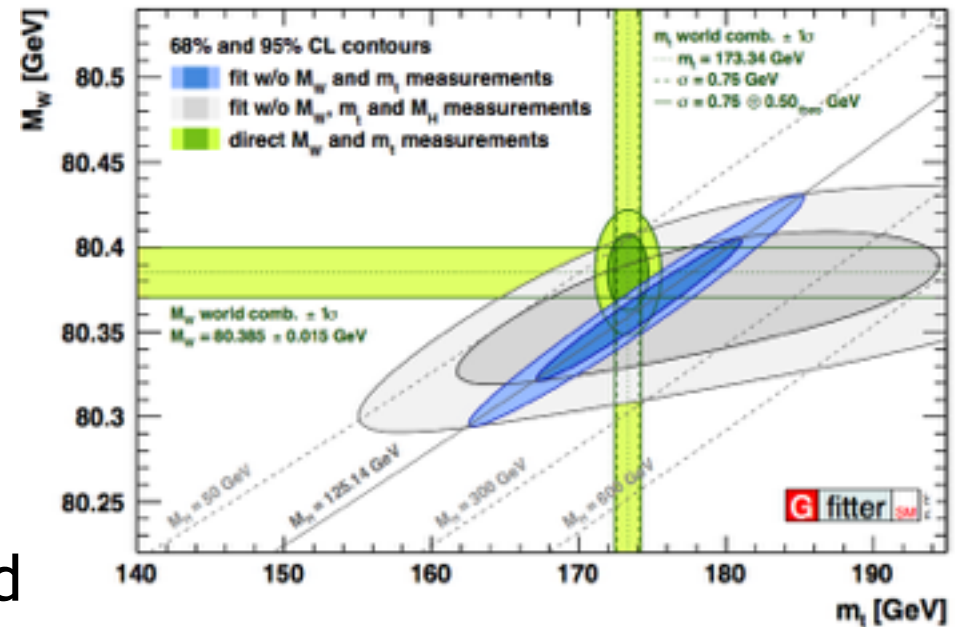
Why care about top mass precision?

- ✓ The only top property not predicted by theory
- ✓ Close to electroweak symmetry breaking scale → impact on precision Higgs physics
- ✓ If there is new physics related to EWSB, top physics is a place to look for

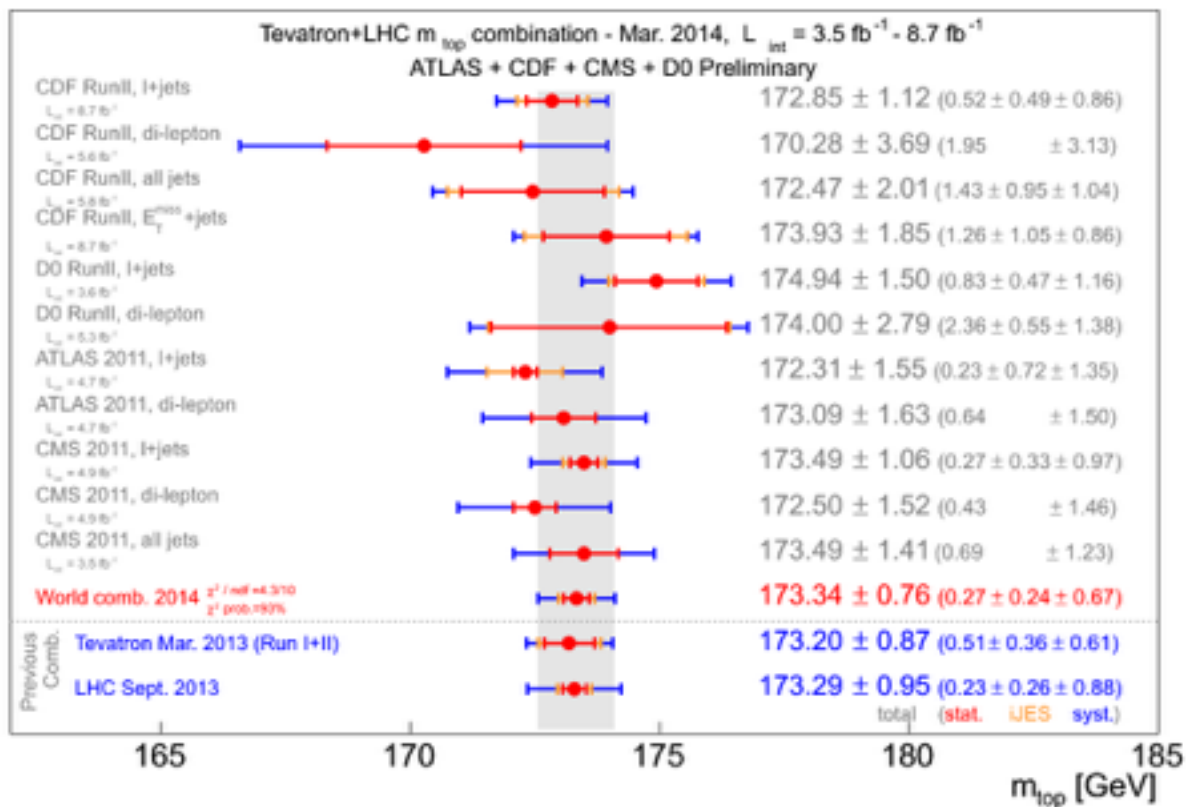


Why care about top mass precision?

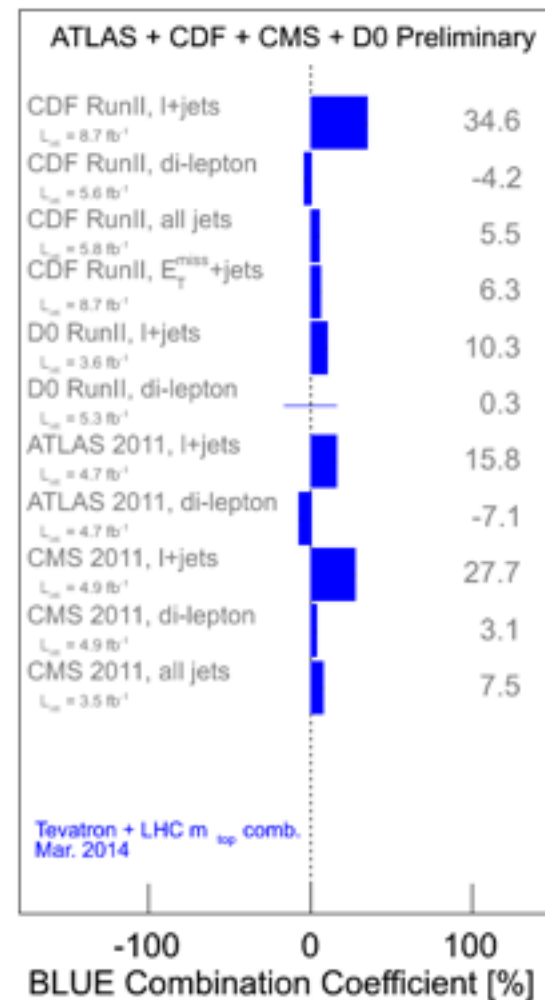
- ✓ The only top property not predicted by theory
- ✓ Close to electroweak symmetry breaking scale → impact on precision Higgs physics
- ✓ If there is new physics related to EWSB, top physics is a place to look for
- ✓ If the SM is assumed valid up to very high scales, the EW vacuum stability depends crucially on the precise top mass value



Status of top mass measurements



0.44% precision



Status of top mass measurements

Results after 2014's World combination

➤ D0 final measurement in lepton+jets:

$$m_t = 174.98 \pm 0.58_{\text{stat+JES}} \pm 0.49_{\text{syst}} \text{ GeV}/c^2 = 174.98 \pm 0.76 \text{ GeV}/c^2$$

PRL **113**, 032002 (2014); PRD **91**, 112003 (2015)

Status of top mass measurements

Results after 2014's World combination

➤ D0 final measurement in lepton+jets:

$$m_t = 174.98 \pm 0.58_{\text{stat+JES}} \pm 0.49_{\text{syst}} \text{ GeV}/c^2 = 174.98 \pm 0.76 \text{ GeV}/c^2$$

PRL 113, 032002 (2014); PRD 91, 112003 (2015)

➤ CMS 7 + 8 TeV measurements in all channels:

$$m_t = 172.35 \pm 0.16_{\text{stat}} \pm 0.48_{\text{syst}} \text{ GeV}/c^2 \text{ (lepton+jets)}$$

$$m_t = 172.32 \pm 0.25_{\text{stat}} \pm 0.59_{\text{syst}} \text{ GeV}/c^2 \text{ (all-jets)}$$

$$m_t = 172.82 \pm 0.19_{\text{stat}} \pm 1.22_{\text{syst}} \text{ GeV}/c^2 \text{ (dilepton)}$$

$$m_t = 172.44 \pm 0.13_{\text{stat}} \pm 0.47_{\text{syst}} \text{ GeV}/c^2 = 172.44 \pm 0.48 \text{ GeV}/c^2$$

PRD 93, 072004 (2016)

0.28% precision!

Status of top mass measurements

Results after 2014's World combination

➤ D0 final measurement in lepton+jets:

$$m_t = 174.98 \pm 0.58_{\text{stat+JES}} \pm 0.49_{\text{syst}} \text{ GeV}/c^2 = 174.98 \pm 0.76 \text{ GeV}/c^2$$

PRL 113, 032002 (2014); PRD 91, 112003 (2015)

➤ CMS 7 + 8 TeV measurements in all channels:

$$m_t = 172.35 \pm 0.16_{\text{stat}} \pm 0.48_{\text{syst}} \text{ GeV}/c^2 \text{ (lepton+jets)}$$

$$m_t = 172.32 \pm 0.25_{\text{stat}} \pm 0.59_{\text{syst}} \text{ GeV}/c^2 \text{ (all-jets)}$$

$$m_t = 172.82 \pm 0.19_{\text{stat}} \pm 1.22_{\text{syst}} \text{ GeV}/c^2 \text{ (dilepton)}$$

$$m_t = 172.44 \pm 0.13_{\text{stat}} \pm 0.47_{\text{syst}} \text{ GeV}/c^2 = 172.44 \pm 0.48 \text{ GeV}/c^2$$

PRD 93, 072004 (2016)

>3 σ difference

New top mass measurement at CDF

P. Bartos	A. Komenius University, Bratislava
G. Bellettini	University of Pisa & Fermilab
L. A. Jimenez-Rugama	Illinois Institute of Technology
S. Mrenna	Fermilab
I. Suslov	JINR Dubna
C. Tosciri	University of Pisa
G. Velev	Fermilab
C. Vellidis	Fermilab
I. Volobouev	Texas Tech University

New top mass measurement at CDF

P. Bartos	A. Komenius University, Bratislava
G. Bellettini	University of Pisa & Fermilab
L. A. Jimenez-Rugama	Illinois Institute of Technology
S. Mrenna	Fermilab
I. Suslov	JINR Dubna
C. Tosciri	University of Pisa (<u>Laurea 05/30/16</u>)
G. Velev	Fermilab
C. Vellidis	Fermilab
I. Volobouev	Texas Tech University

New top mass measurement at CDF

P. Bartos	A. Komenius University, Bratislava
G. Bellettini	University of Pisa & Fermilab
L. A. Jimenez-Rugama	Illinois Institute of Technology
S. Mrenna	Fermilab
I. Suslov	JINR Dubna
C. Tosciri	University of Pisa (<u>Laurea 05/30/16</u>)
G. Velev	Fermilab
C. Vellidis	Fermilab
I. Volobouev	Texas Tech University

Last top mass measurement from CDF, aiming to:

- ◇ Reach highest possible precision from CDF data
- ◇ Examine tension between “low” LHC and “high” Tevatron results

Definition of top pair candidate event

- ✓ One and only good lepton: central electron / tight or loose muon
- ✓ At least 4 jets, reconstructed with a cone algorithm (JetClu) of radius $R = \sqrt{(\Delta\eta)^2 + (\Delta\phi)^2} = 0.4$
- ✓ A number of b-jet tags, varying by candidate event category, using a secondary vertex algorithm (SecVtx)
- ✓ Large missing E_T , reflecting the presence of a neutrino from the leptonic W boson decay in the final state

“Tight” and “loose” event selection

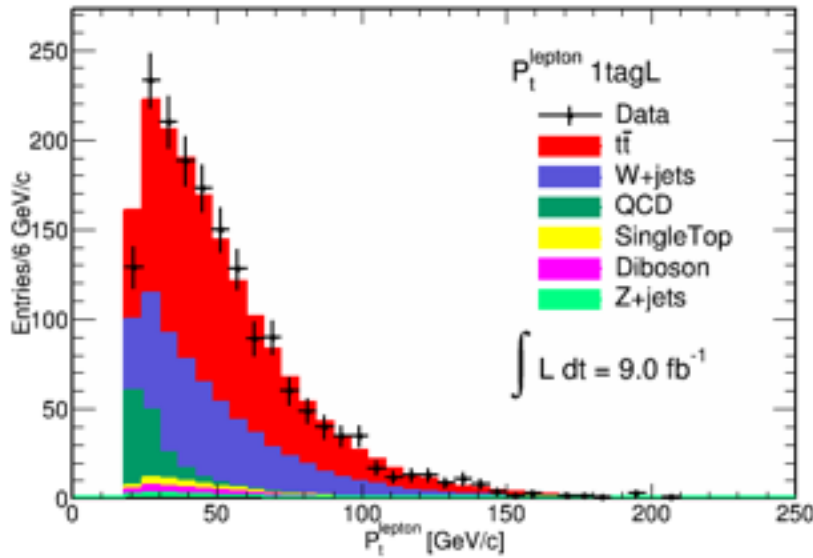
- ✓ Tight jet: $E_T > 20$ GeV, $|\eta| < 2.0$
- ✓ Loose jet: $E_T > 12$ GeV, $|\eta| < 2.4$
- ✓ Tight selection: events with exactly 4 tight jets and any loose jets
- ✓ Loose selection: events with ≥ 3 T jets + ≥ 1 L jet
- ✓ Categories by selection/b-tags: 0-tag, 1-tagL, 1-tagT, 2-tagL, 2-tagT

Physics processes and simulation models

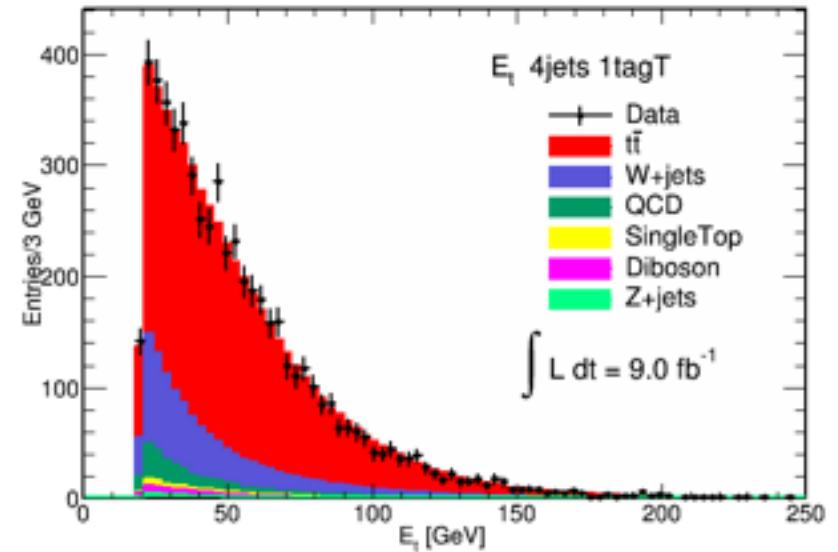
- $t\bar{t}$ signal: Powheg + Pythia, S. Frixione *et al.*, JHEP07, 0709 (2007)
- W/Z + jets: Alpgen+Pythia, M.L. Mangano *et al.*, JHEP0307:001 (2003)
- Dibosons: Pythia 6, T. Sjöstrand *et al.*, JHEP06, 026 (2006)
- Single top: Madgraph 4 + Pythia, J. Alwall *et al.*, JHEP09, 028 (2007)
- QCD: data with lepton failing one of the “good lepton” criteria
- All MC samples processed through the standard CDF detector simulation and event reconstruction software, E. Gerchtein and M. Paulini, arXiv:physics/0306031 (2003)

Kinematic spectra

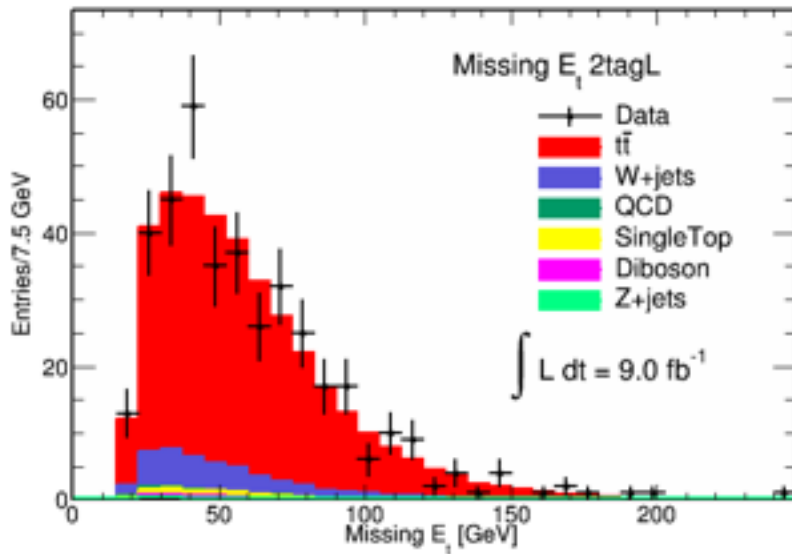
CDF Preliminary



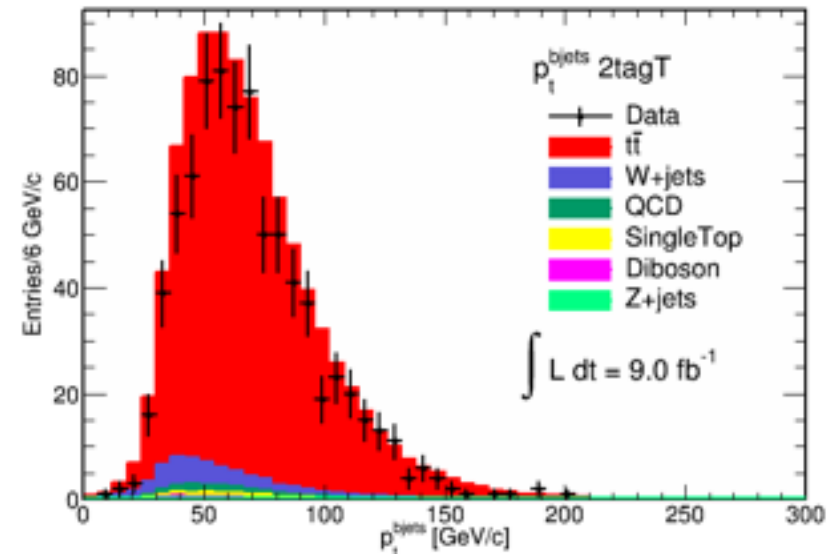
CDF Preliminary



CDF Preliminary

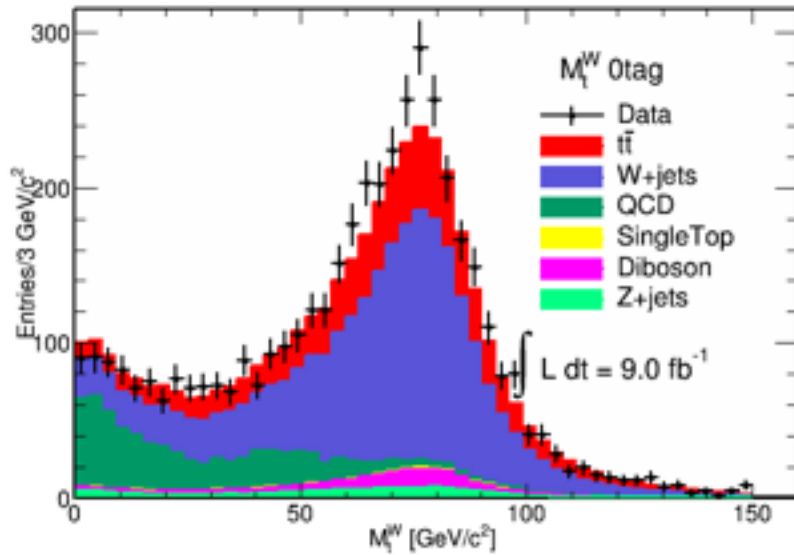


CDF Preliminary

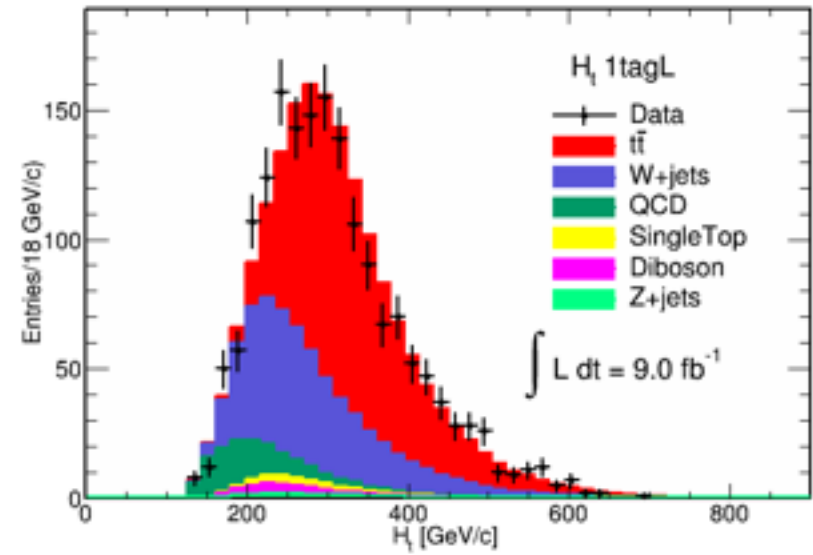


Kinematic spectra

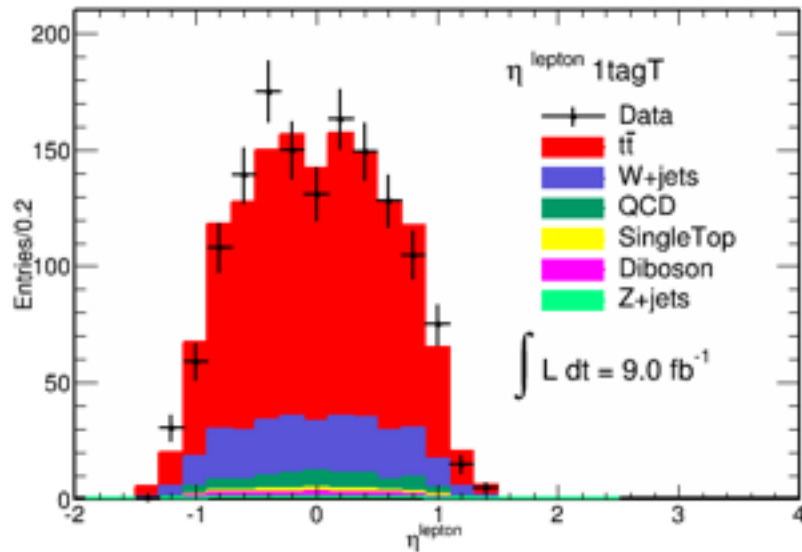
CDF Preliminary



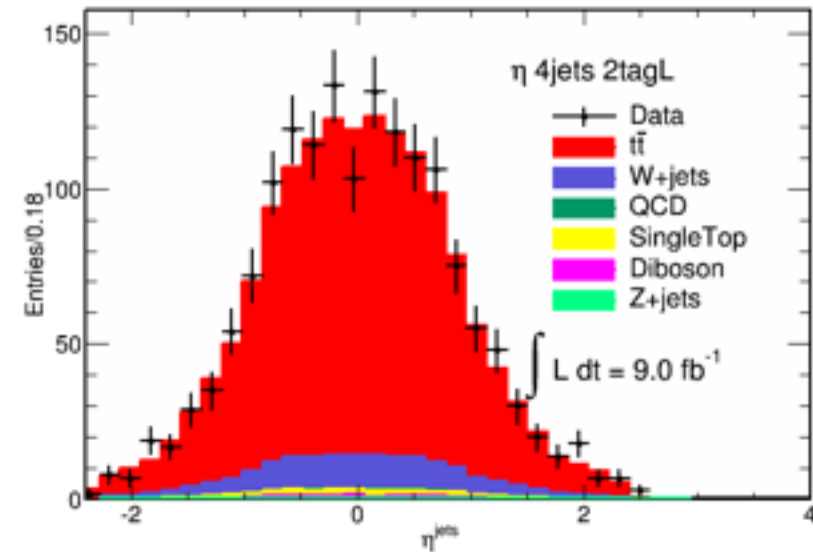
CDF Preliminary



CDF Preliminary



CDF Preliminary



Improvements relative to the previous measurement

- More luminosity: from 5.6 fb^{-1} to 9 fb^{-1} → 60% more data
- New candidate categories: 0-tag, 1-tagL, 2-tagL → 30% more candidate events from loose categories
- New matrix element integration method, allowing for reliable error estimation → higher integration accuracy
- NLO singal MC: Powheg + Pythia → reduction of uncertainty from higher-order terms

The matrix element method

- ✓ Based on the use of the m_t dependence of the top quark pair production cross section through the maximization of a suitable likelihood function

$$L = \prod_{i=1}^N \left(\frac{N_s}{N} L_i^s + \frac{N_b}{N} L_i^b \right)$$

The matrix element method

- ✓ Based on the use of the m_t dependence of the top quark pair production cross section through the maximization of a suitable likelihood function

$$L = \prod_{i=1}^N \left(\frac{N_s}{N} L_i^s + \frac{N_b}{N} L_i^b \right)$$

- ✓ Provides maximal statistical sensitivity by exploiting the full topological and kinematic information of each event
- ✓ Idea conceived already in Tevatron Run I, repeatedly applied by both Tevatron experiments in all top quark pair decay channels and many versions for various measurements
- ✓ Last applied by CDF in lepton+jets using 5.6 fb^{-1} , most precise single m_t measurement at the time, PRL **105**, 252001 (2010)
- ✓ Last applied by D0 in lepton+jets using 9.7 fb^{-1} , most precise single m_t measurement at the time, PRL **113**, 032002 (2014)

In situ JES calibration

Choose a m_t estimator which is also sensitive to m_W , so that a shift of the mass of the hadronically decaying W from the peak due to the JES uncertainty induces a large change of the estimator

In situ JES calibration

Choose a m_t estimator which is also sensitive to m_W , so that a shift of the mass of the hadronically decaying W from the peak due to the JES uncertainty induces a large change of the estimator

$$L_i^s(m_t, \Delta_{JES}) \propto P(\vec{x}_i | m_t, \Delta_{JES})$$

$$JES = \frac{p_T^{Calor-jet}}{p_T^{MC-jet}} = 1 + \Delta_{JES} \sigma_{JES}(\vec{p}^{jet})$$

- Define the likelihood as a 2-variable function of m_t and Δ_{JES}
- $\Delta_{JES}=0$ defines the nominal JES
- $P(x_i | m_t, \Delta_{JES})$ strongly dependent on m_W and maximal at the m_W peak

Definition of the likelihood

$$L_i^s(m_t, \Delta_{JES}) = \frac{1}{N(m_t)} \frac{1}{A(m_t, \Delta_{JES})} \sum_{j=1}^{24} w_{ij} P(\vec{x}_i | m_t, \Delta_{JES})$$

Event likelihood

Cross section

Acceptance

Event probability

Definition of the likelihood

$$L_i^s(m_t, \Delta_{JES}) = \frac{1}{N(m_t)} \frac{1}{A(m_t, \Delta_{JES})} \sum_{j=1}^{24} w_{ij} P(\vec{x}_i | m_t, \Delta_{JES})$$

$$P(\vec{x} | m_t, \Delta_{JES}) = \int T(\vec{x} | \vec{y}, \Delta_{JES}) \left| M_{2p \rightarrow lv_1+4p}^{t\bar{t}}(m_t, \vec{y}) \right|^2 \times \frac{f(z_1, Q^2) f(z_2, Q^2)}{z_1 z_2} \Big|_{Q=2m_t} dz_1 dz_2 d\Phi(\vec{y})$$

Definition of the likelihood

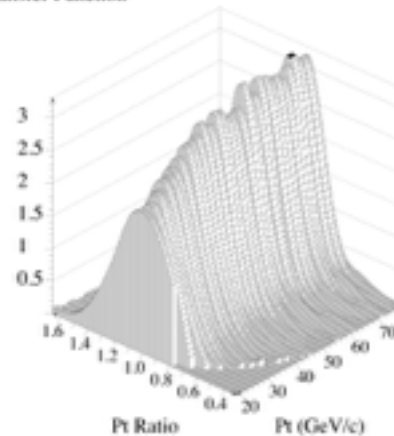
$$L_i^s(m_t, \Delta_{JES}) = \frac{1}{N(m_t)} \frac{1}{A(m_t, \Delta_{JES})} \sum_{j=1}^{24} w_{ij} P(\vec{x}_i | m_t, \Delta_{JES})$$

$$P(\vec{x} | m_t, \Delta_{JES}) = \int T(\vec{x} | \vec{y}, \Delta_{JES}) \left| M_{2p \rightarrow lv_1+4p}^{t\bar{t}}(m_t, \vec{y}) \right|^2 \times \frac{f(z_1, Q^2) f(z_2, Q^2)}{z_1 z_2} \Big|_{Q=2m_t} dz_1 dz_2 d\Phi(\vec{y})$$

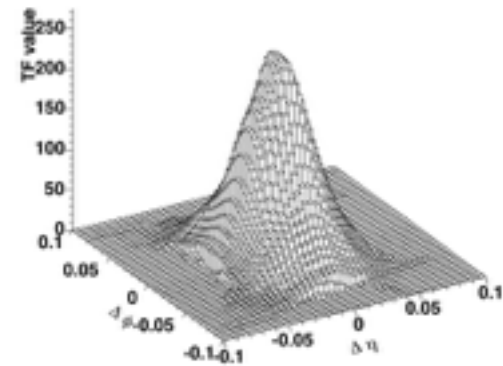
From MC, separately for b & light jets

$$T = F_1\left(\frac{p_T^j}{p_T^p}, p_T^p, \eta_p, m\right) \times F_2(\Delta\eta_{j-p}, \Delta\phi_{j-p}, p_T^p, \eta_p, m)$$

Transfer Function



Light quark angular transfer function, $\eta_j = 0$, $m = 5$



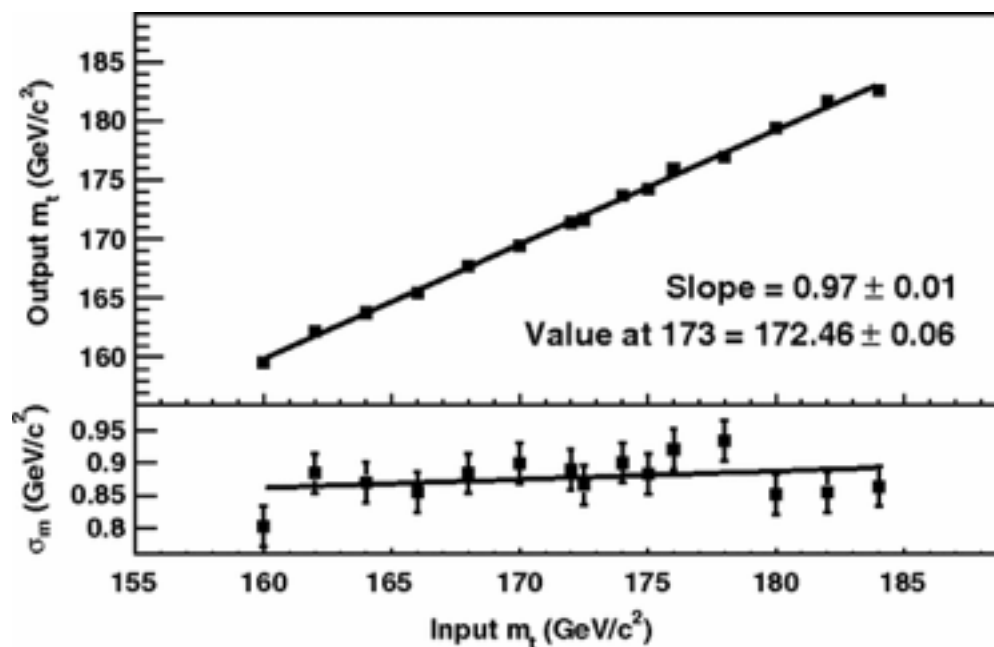
PRL 105, 252001 (2010)

Method calibration

- ◇ Use joint signal+background $L(m_t, \Delta_{JES})$ in pseudo-experiments (PEs)
- ◇ Run PEs with Poisson average equal to the expected candidate events
- ◇ Find average m_t , bias, expected σ_m , pull width for the PE ensemble
- ◇ Correct for any bias in m_t and σ_m ; apply similar procedure for Δ_{JES}
- ◇ Treat Δ_{JES} as nuisance to measure m_t from $L_{prof}(m_t) = \max_{\Delta_{JES}} L(m_t, \Delta_{JES})$

Method calibration

- ◇ Use joint signal+background $L(m_t, \Delta_{JES})$ in pseudo-experiments (PEs)
- ◇ Run PEs with Poisson average equal to the expected candidate events
- ◇ Find average m_t , bias, expected σ_m , pull width for the PE ensemble
- ◇ Correct for any bias in m_t and σ_m ; apply similar procedure for Δ_{JES}
- ◇ Treat Δ_{JES} as nuisance to measure m_t from $L_{prof}(m_t) = \max_{\Delta_{JES}} L(m_t, \Delta_{JES})$



From PRL 105, 252001

Systematic uncertainties

PRL 105, 252001
(2010)

Systematic source	Uncertainty (GeV/
<i>Calibration</i>	<i>0.10</i>
<i>MC generator</i>	<i>0.37</i>
<i>Initial/final state</i>	<i>0.15</i>
<i>Residual JES</i>	<i>0.49</i>
<i>b-JES</i>	<i>0.26</i>
<i>Lepton p_T</i>	<i>0.14</i>
<i>Multiple collisions</i>	<i>0.10</i>
<i>PDF</i>	<i>0.14</i>
<i>Background</i>	<i>0.33</i>
<i>Color reconnection</i>	<i>0.37</i>
Total	0.88

Systematic uncertainties


Systematic source	Uncertainty (GeV/
<i>Calibration</i>	<i>0.10</i>
<i>MC generator</i>	<i>0.37</i>
<i>Initial/final state</i>	<i>0.15</i>
<i>Residual JES</i>	<i>0.49</i>
<i>b-JES</i>	<i>0.26</i>
<i>Lepton p_T</i>	<i>0.14</i>
<i>Multiple collisions</i>	<i>0.10</i>
<i>PDF</i>	<i>0.14</i>
<i>Background</i>	<i>0.33</i>
<i>Color reconnection</i>	<i>0.37</i>
Total	0.88

Remove overlap
from hadronization


Systematic uncertainties

Systematic source	Uncertainty (GeV/
<i>Calibration</i>	<i>0.10</i>
<i>MC generator</i>	<i>0.37</i>
<i>Initial/final state</i>	<i>0.15</i>
<i>Residual JES</i>	<i>0.49</i>
<i>b-JES</i>	<i>0.26</i>
<i>Lepton p_T</i>	<i>0.14</i>
<i>Multiple collisions</i>	<i>0.10</i>
<i>PDF</i>	<i>0.14</i>
<i>Background</i>	<i>0.33</i>
<i>Color reconnection</i>	<i>0.37</i>
<i>Total</i>	<i>0.88</i>

Remove overlap
from hadronization




Reduce by using
a background ℓ



Systematic uncertainties

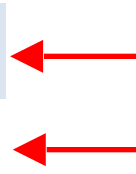
Systematic source	Uncertainty (GeV/
<i>Calibration</i>	<i>0.10</i>
<i>MC generator</i>	<i>0.37</i>
<i>Initial/final state</i>	<i>0.15</i>
<i>Residual JES</i>	<i>0.49</i>
<i>b-JES</i>	<i>0.26</i>
<i>Lepton p_T</i>	<i>0.14</i>
<i>Multiple collisions</i>	<i>0.10</i>
<i>PDF</i>	<i>0.14</i>
<i>Background</i>	<i>0.33</i>
<i>Color reconnection</i>	<i>0.37</i>
<i>Total</i>	<i>0.88</i>

Remove overlap
from hadronization



Reduce by using
a background ℓ

Remove by using
new signal MC



Summary

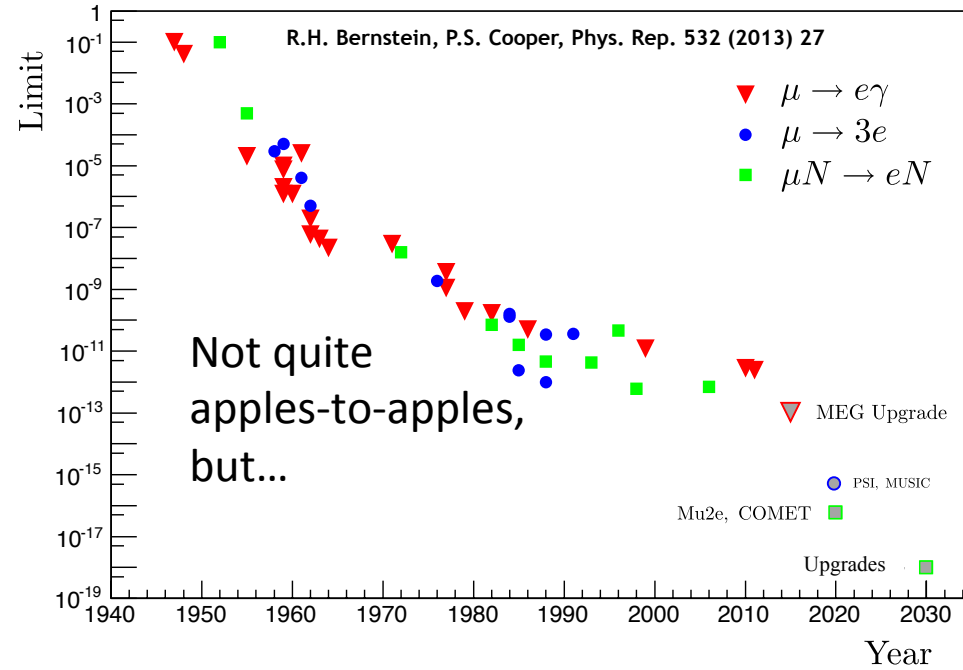
- ◇ CDF top program concludes with a high precision measurement
- ◇ Using **full sample** (9 fb^{-1}) & **matrix element** (optimal) technique
- ◇ Revisiting dominant systematic uncertainties
- ◇ Last word, **most precise** top mass result from CDF
- ◇ Expected to be included in next World average

The Mu2e experiment at Fermilab:
Search for neutrinoless muon-to-electron
conversion

Charged lepton flavor violation

- While flavor mixing is observed in the quark and neutrino sectors, Charged Lepton Flavor Violation (CLFV) has never so far been observed
- CLFV is a nearly universal feature of Standard Model extensions
- CLFV is a powerful probe of multi-TeV scale dynamics: complementary to direct collider searches
- Among various possible CLFV modes to search for, rare muon processes offer best combination of new physics reach and experimental sensitivity

History of CLFV searches with μ



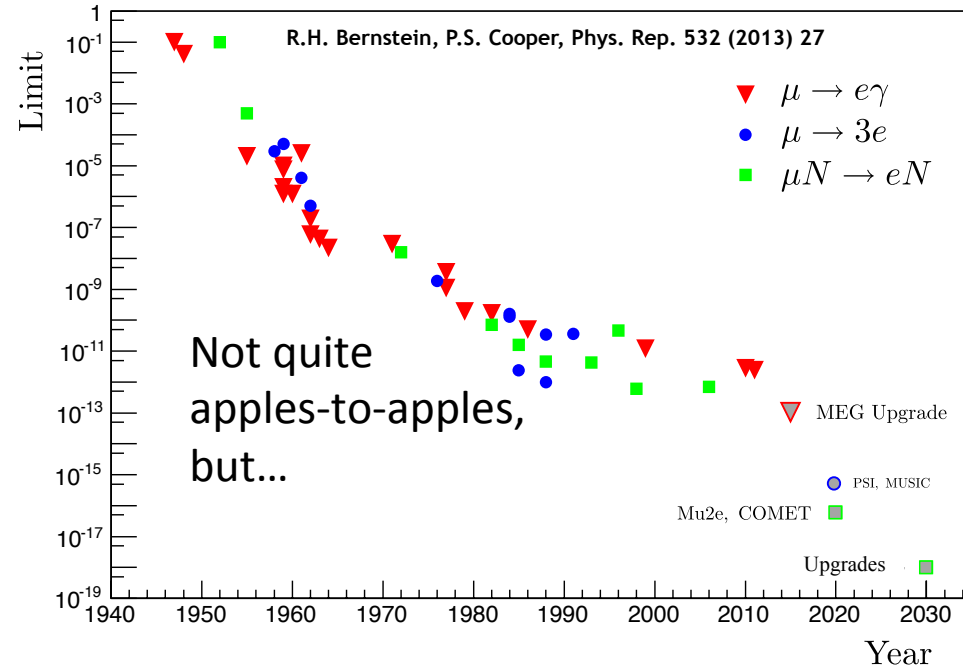
Best 90% C.L. limits

$$R_{\mu e} < 7 \times 10^{-13} \text{ (Sindrum-II 2006)}$$

$$\text{Br}(\mu \rightarrow e\gamma) < 4.2 \times 10^{-13} \text{ (MEG 2016)}$$

$$\text{Br}(\mu \rightarrow 3e) < 1 \times 10^{-12} \text{ (Sindrum-I 1988)}$$

History of CLFV searches with μ



Best 90% C.L. limits

$$R_{\mu e} < 7 \times 10^{-13} \text{ (Sindrum-II 2006)}$$

$$\text{Br}(\mu \rightarrow e\gamma) < 4.2 \times 10^{-13} \text{ (MEG 2016)}$$

$$\text{Br}(\mu \rightarrow 3e) < 1 \times 10^{-12} \text{ (Sindrum-I 1988)}$$

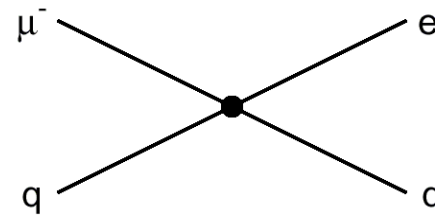
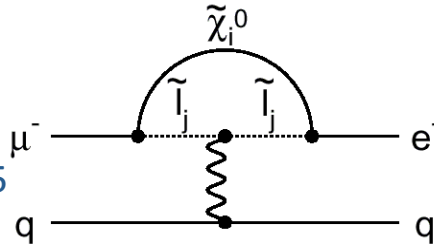
Mu2e will measure:

$$R_{\mu e} \equiv \frac{\Gamma(\mu^- N(A, Z) \rightarrow e^- + N(A, Z))}{\Gamma(\mu^- N(A, Z) \rightarrow \nu_\mu + N'(A, Z-1))}$$

Goal: single event sensitivity of $R_{\mu e} = \text{“a few”} \times 10^{-17}$

*Example sensitivities of $\mu+N \rightarrow e+N$

Supersymmetry
Predictions at 10^{-15}

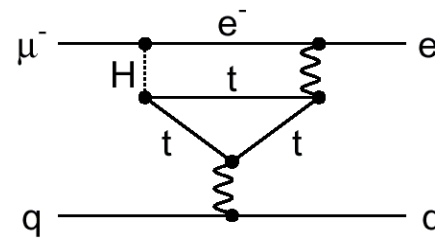
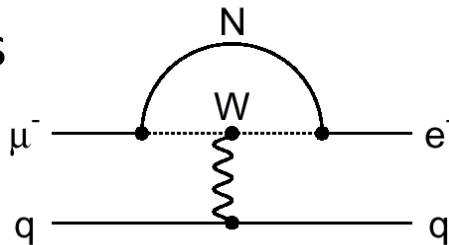


Compositeness

$$\Lambda_c = 3000 \text{ TeV}$$

Heavy Neutrinos

$$|U_{\mu N}^* U_{eN}|^2 = 8 \times 10^{-13}$$

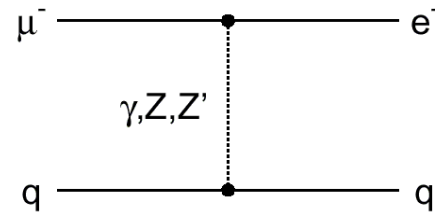
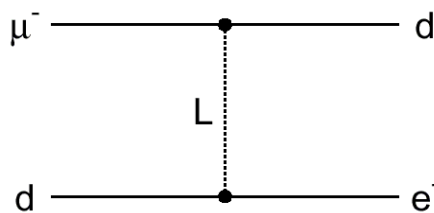


Second Higgs
doublet

$$g_{H\mu e} = 10^{-4} \times g_{H\mu\mu}$$

Leptoquarks

$$M_L = 3000 \sqrt{\lambda_{\mu d} \lambda_{e d}} \text{ TeV}/c^2$$



Heavy Z' ,
Anomalous Z
coupling

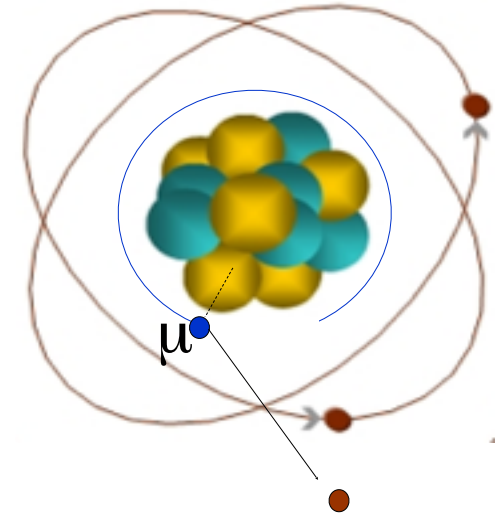
$$M_{Z'} = 3000 \text{ TeV}/c^2$$

$$B(Z \rightarrow \mu e) < 10^{-17}$$

*After W. Marciano

Experimental signature of $\mu+N \rightarrow e+N$

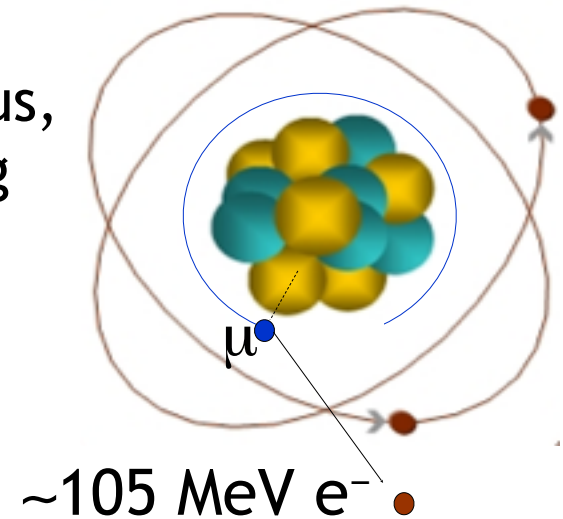
- ◇ A muon captured by a nucleus has an enhanced probability of decay by the exchange of a virtual particle with the nucleus



Experimental signature of $\mu+N \rightarrow e+N$

- ◇ A muon captured by a nucleus has an enhanced probability of decay by the exchange of a virtual particle with the nucleus
- ◇ This reaction recoils against the entire nucleus, producing a *mono-energetic* electron carrying most of the muon rest energy

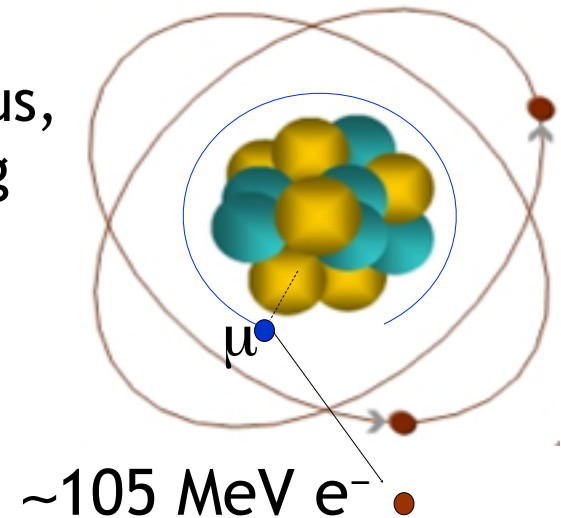
$$E_e = m_\mu c^2 - \frac{(m_e c^2)^2}{2m_N c^2}$$



Experimental signature of $\mu+N \rightarrow e+N$

- ◇ A muon captured by a nucleus has an enhanced probability of decay by the exchange of a virtual particle with the nucleus
- ◇ This reaction recoils against the entire nucleus, producing a *mono-energetic* electron carrying most of the muon rest energy

$$E_e = m_\mu c^2 - \frac{(m_e c^2)^2}{2m_N c^2}$$



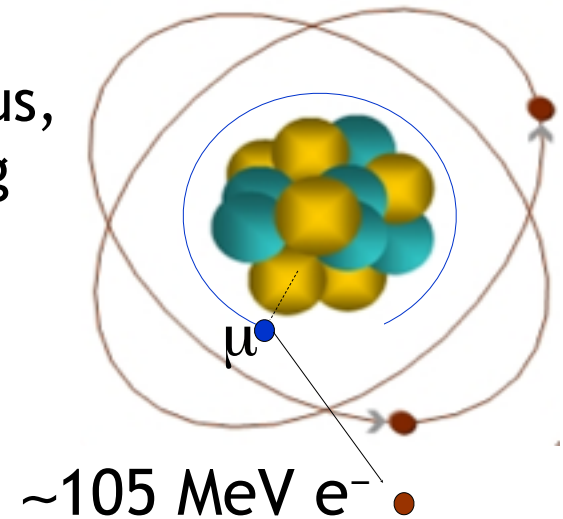
➤ Similar to $\mu \rightarrow e\gamma$, with important advantages:

- ✓ No combinatorial background
- ✓ Because the virtual particle can be a photon *or* heavy neutral boson, this reaction is sensitive to a broader range of new physics

Experimental signature of $\mu+N \rightarrow e+N$

- ◇ A muon captured by a nucleus has an enhanced probability of decay by the exchange of a virtual particle with the nucleus
- ◇ This reaction recoils against the entire nucleus, producing a *mono-energetic* electron carrying most of the muon rest energy

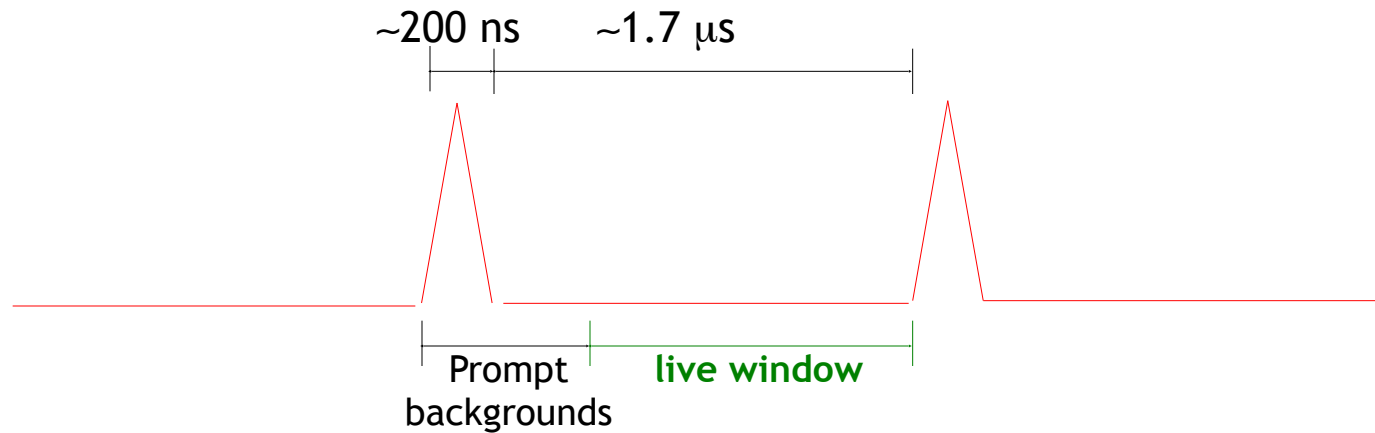
$$E_e = m_\mu c^2 - \frac{(m_e c^2)^2}{2m_N c^2}$$



- Similar to $\mu \rightarrow e\gamma$, with important advantages:
 - ✓ No combinatorial background
 - ✓ Because the virtual particle can be a photon *or* heavy neutral boson, this reaction is sensitive to a broader range of new physics
- The relative rate of $\mu \rightarrow e\gamma$ and $\mu N \rightarrow eN$ is the most important clue regarding the details of the physics

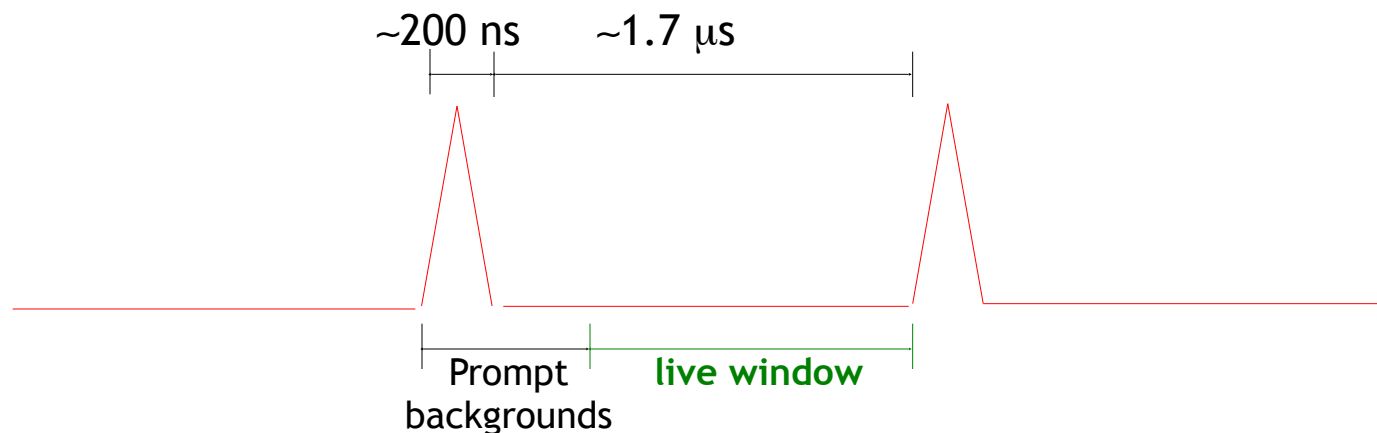
Mu2e experimental technique

- Eliminate prompt beam backgrounds by using a primary beam consisting of short proton pulses with separation on the order of a muon life time



Mu2e experimental technique

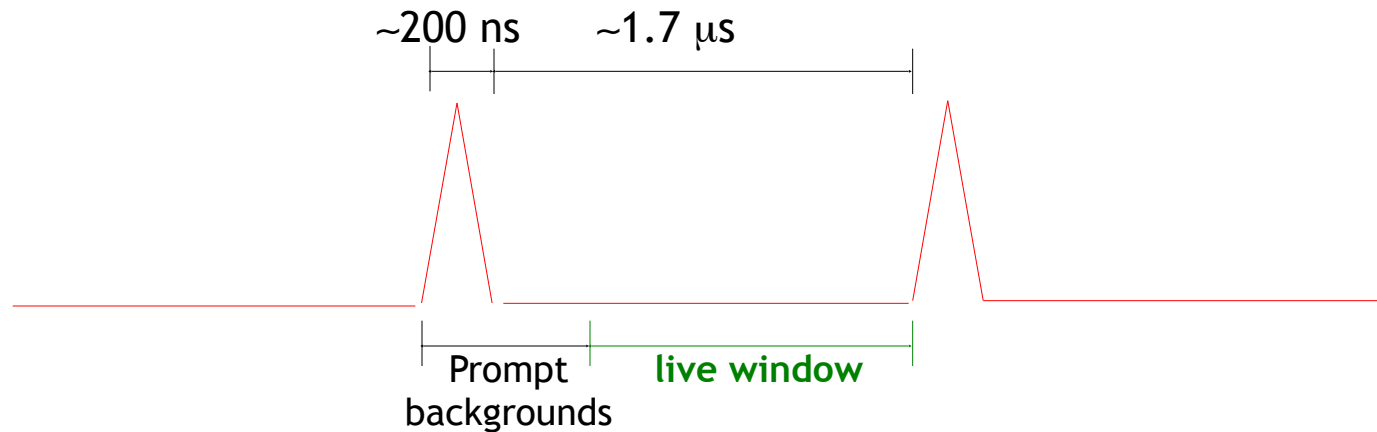
- Eliminate prompt beam backgrounds by using a primary beam consisting of short proton pulses with separation on the order of a muon life time



- Design a transport channel to optimize the transport of right-sign, low momentum muons from the production target to the muon capture target

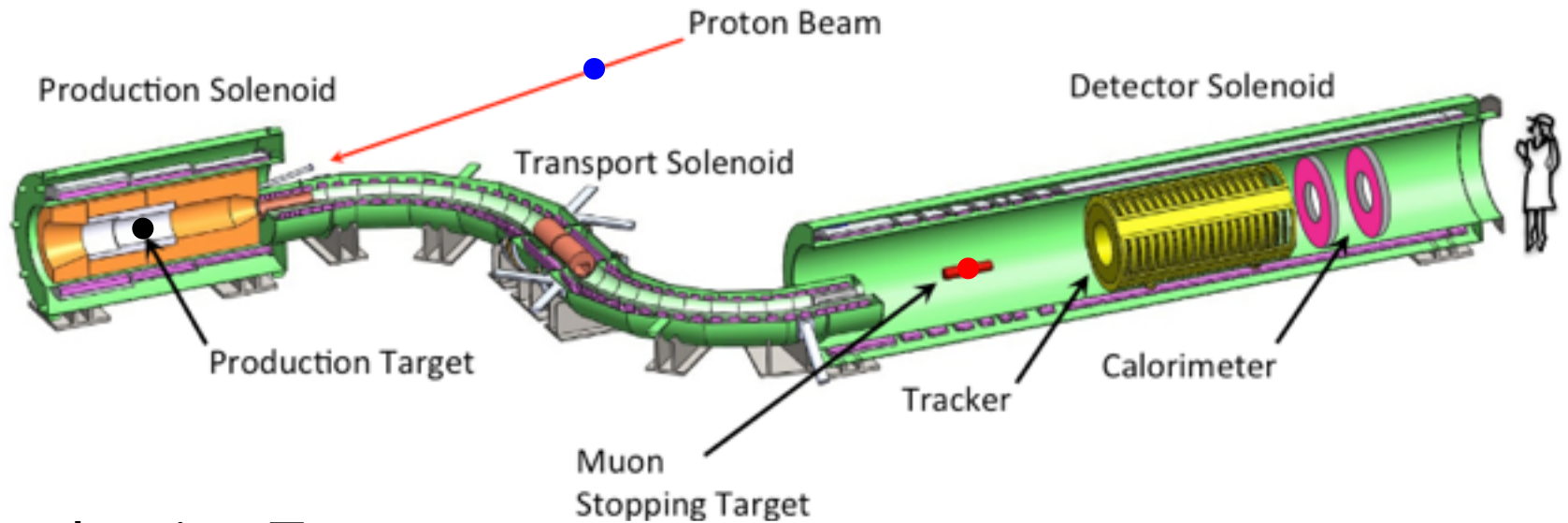
Mu2e experimental technique

- Eliminate prompt beam backgrounds by using a primary beam consisting of short proton pulses with separation on the order of a muon life time



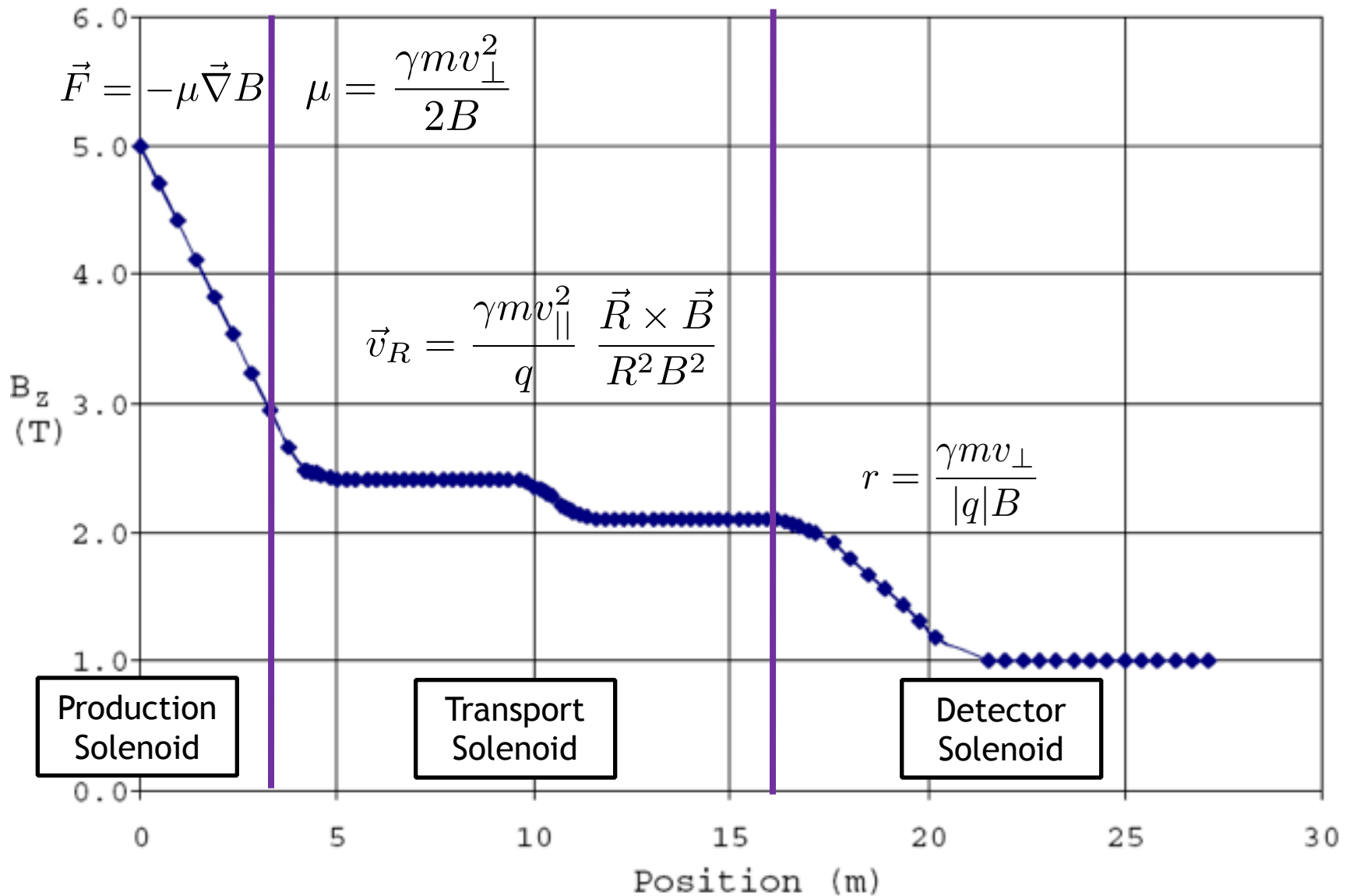
- Design a transport channel to optimize the transport of right-sign, low momentum muons from the production target to the muon capture target
- Design a detector which is very insensitive to electrons from ordinary muon decays

Muon beamline and Mu2e detector



- Production Target
 - ✓ Proton beam strikes target, producing mostly pions
- Production Solenoid
 - ✓ Contains backward pions/muons and reflects slow forward pions/muons
- Transport Solenoid
 - ✓ Selects low momentum, negative muons
- Capture Target, Detector, and Detector Solenoid
 - ✓ Capture muons on Aluminum target and wait for them to decay
 - ✓ Detector blind to ordinary (Michel) decays, with $E \leq \frac{1}{2}m_{\mu}c^2$
 - ✓ Optimized for $E \sim m_{\mu}c^2$

Magnetic field



Field testing

- Field simulation model uses a 3D grid (field map) per solenoid
 - ✓ Field evaluated by 3D interpolation at any given point
 - ✓ Field maps provided by constructors for every new design

Field testing

- Field simulation model uses a 3D grid (field map) per solenoid
 - ✓ Field evaluated by 3D interpolation at any given point
 - ✓ Field maps provided by constructors for every new design
- Every new set of field maps is tested against the previous one
 - ✓ Verify differences with previous design are within tolerance
 - ✓ Verify criteria required by the update are met

Field testing

- Field simulation model uses a 3D grid (field map) per solenoid
 - ✓ Field evaluated by 3D interpolation at any given point
 - ✓ Field maps provided by constructors for every new design
- Every new set of field maps is tested against the previous one
 - ✓ Verify differences with previous design are within tolerance
 - ✓ Verify criteria required by the update are met
- Toolkit for field map validation developed (F. Bradascio)
 - ✓ Variety of 3D interpolation algorithms for precision tests
 - ✓ Plotting package for field and gradient plots
 - ✓ Analysis package mapping differences on the experiment geometry and scanning their importance

Implications of field uncertainties (from coil misalignments)

- Stopping rates:
 - ✓ Uncertain μ^- flux on capture target
 - ✓ Uncertain π^- flux on capture target (background)

Implications of field uncertainties (from coil misalignments)

- Stopping rates:
 - ✓ Uncertain μ^- flux on capture target
 - ✓ Uncertain π^- flux on capture target (background)
- Background from beam electrons:
 - ✓ Uncertain high-momentum e^- flux coming with the beam
 - ✓ Background source (signal-like scattering into the detector)

Implications of field uncertainties (from coil misalignments)

- Stopping rates:
 - ✓ Uncertain μ^- flux on capture target
 - ✓ Uncertain π^- flux on capture target (background)
- Background from beam electrons:
 - ✓ Uncertain high-momentum e^- flux coming with the beam
 - ✓ Background source (signal-like scattering into the detector)
- β^- source test:
 - ✓ Low-momentum particles follow closely magnetic field lines
 - ✓ Use electrons from a β^- source to trace field lines
 - ✓ Test very sensitive to coil misalignments

Implications of field uncertainties (from coil misalignments)

- Stopping rates:
 - ✓ Uncertain μ^- flux on capture target
 - ✓ Uncertain π^- flux on capture target (background)
- Background from beam electrons:
 - ✓ Uncertain high-momentum e^- flux coming with the beam
 - ✓ Background source (signal-like scattering into the detector)
- β^- source test:
 - ✓ Low-momentum particles follow closely magnetic field lines
 - ✓ Use electrons from a β^- source to trace field lines
 - ✓ Test very sensitive to coil misalignments

Studied with misaligned coil simulations

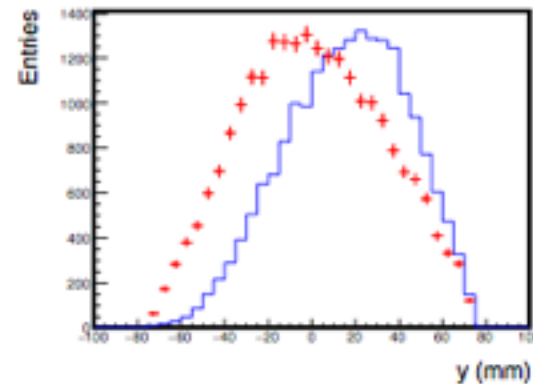
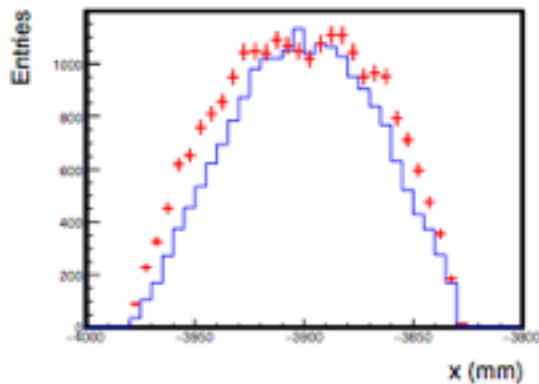
Implications of field uncertainties (from coil misalignments)

➤ Stopping rates:

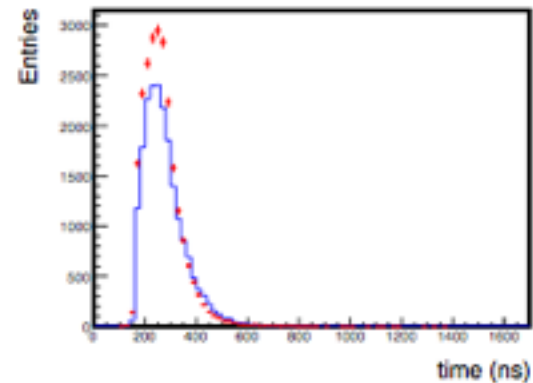
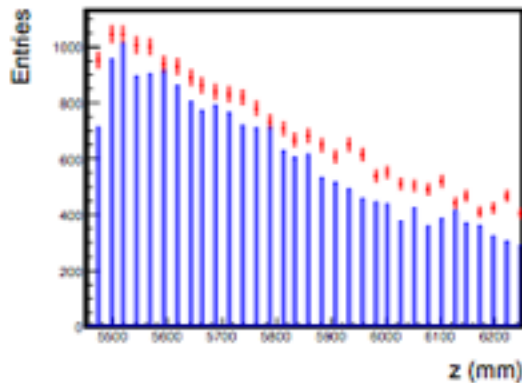
✓ Uncertain μ^- flux on capture target

✓ Uncertain π^- flux on capture target (background)

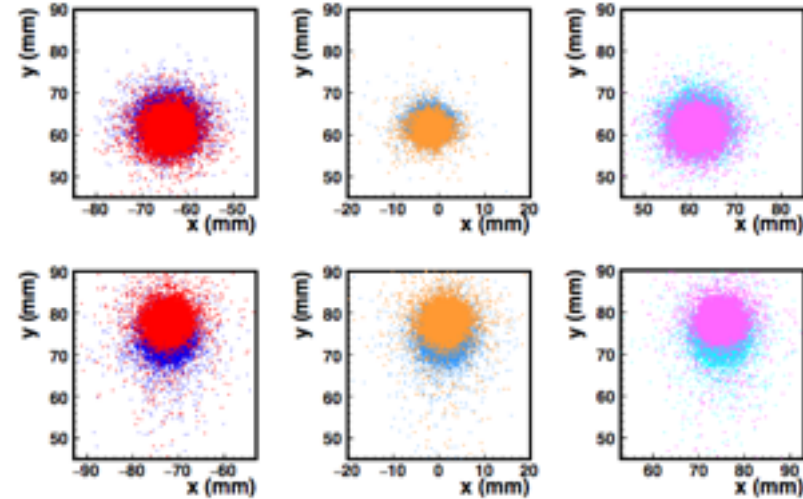
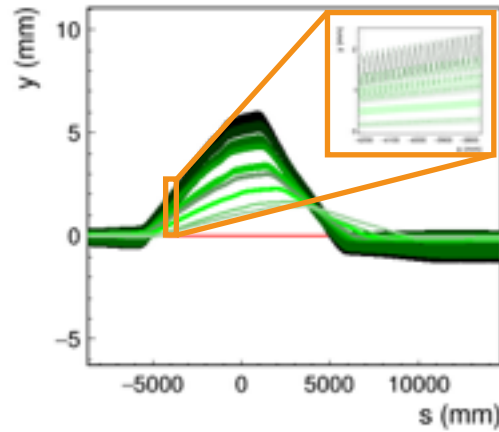
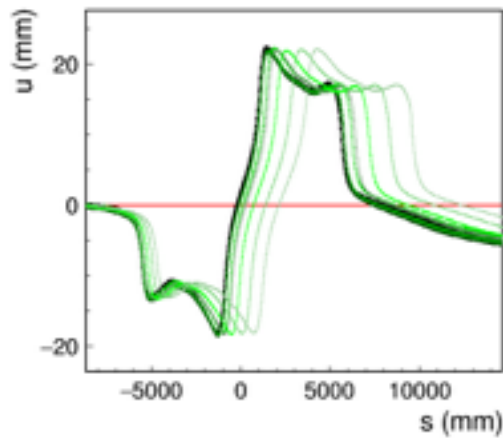
F. Bradascio, Laurea
University of Pisa



Stopped π^- distributions for exaggerated misalignment (blue histograms)



Implications of field uncertainties (from coil misalignments)



➤ β^- source test:

- ✓ Low-momentum particles follow closely magnetic field lines
- ✓ Use electrons from a β^- source to trace field lines
- ✓ Test very sensitive to coil misalignments

F. Bradascio, Laurea
University of Pisa

Summary

- Mu2e will measure the ratio of coherent $\mu \rightarrow e$ conversions in the field of a nucleus to ordinary μ captures with an initial *single event sensitivity of $R_{\mu e} \sim 3 \times 10^{-17}$*

Summary

- Mu2e will measure the ratio of coherent $\mu \rightarrow e$ conversions in the field of a nucleus to ordinary μ captures with an initial ***single event sensitivity of $R_{\mu e} \sim 3 \times 10^{-17}$***
- This represents an improvement of ***four orders of magnitude*** compared to the existing limit, or over a ***factor of ten*** in effective mass reach

Summary

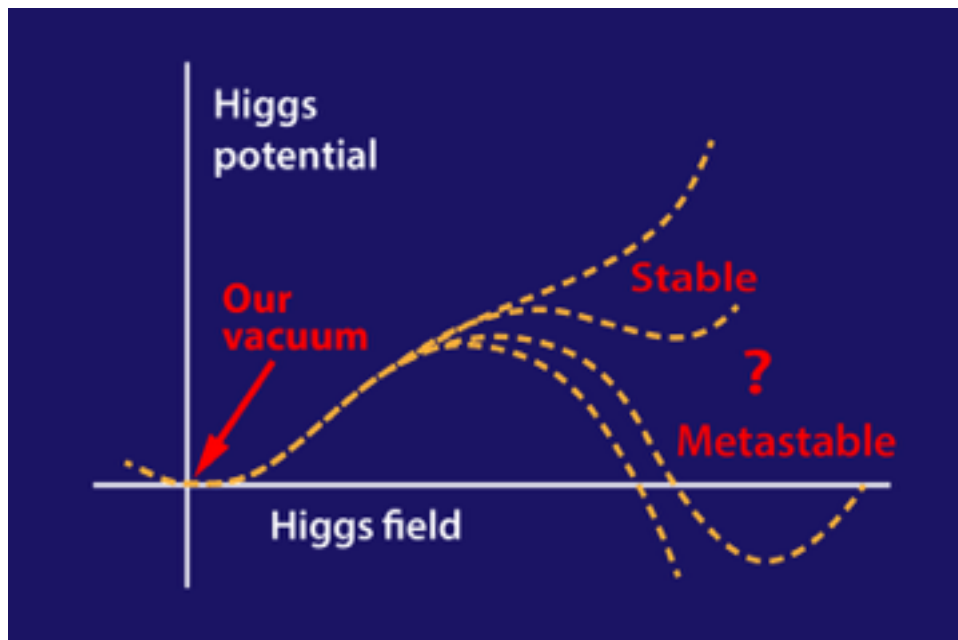
- ❑ Mu2e will measure the ratio of coherent $\mu \rightarrow e$ conversions in the field of a nucleus to ordinary μ captures with an initial ***single event sensitivity of $R_{\mu e} \sim 3 \times 10^{-17}$***
- ❑ This represents an improvement of ***four orders of magnitude*** compared to the existing limit, or over a ***factor of ten*** in effective mass reach
- ❑ The experiment is designed to operate at a point in instrumental parameter space satisfying the precision requirements to achieve the target sensitivity

Summary

- Mu2e will measure the ratio of coherent $\mu \rightarrow e$ conversions in the field of a nucleus to ordinary μ captures with an initial ***single event sensitivity of $R_{\mu e} \sim 3 \times 10^{-17}$***
- This represents an improvement of ***four orders of magnitude*** compared to the existing limit, or over a ***factor of ten*** in effective mass reach
- The experiment is designed to operate at a point in instrumental parameter space satisfying the precision requirements to achieve the target sensitivity
- Field studies have shown that the design operating point is stable, by demonstrating that relevant physics quantities (stopping rates, background expectations) are insensitive to field uncertainties from realistic solenoid misalignments

Top mass backup

Stability of the Higgs potential



- ◇ Interplay of the Higgs field mass and self-coupling terms shapes the Higgs potential
- ◇ For some Higgs and top mass values, the Higgs potential can go negative at very short distances, allowing tunneling to a lower-energy state than the present minimum (vacuum)
- ◇ Metastability scenarios are related to inflation

The Tevatron

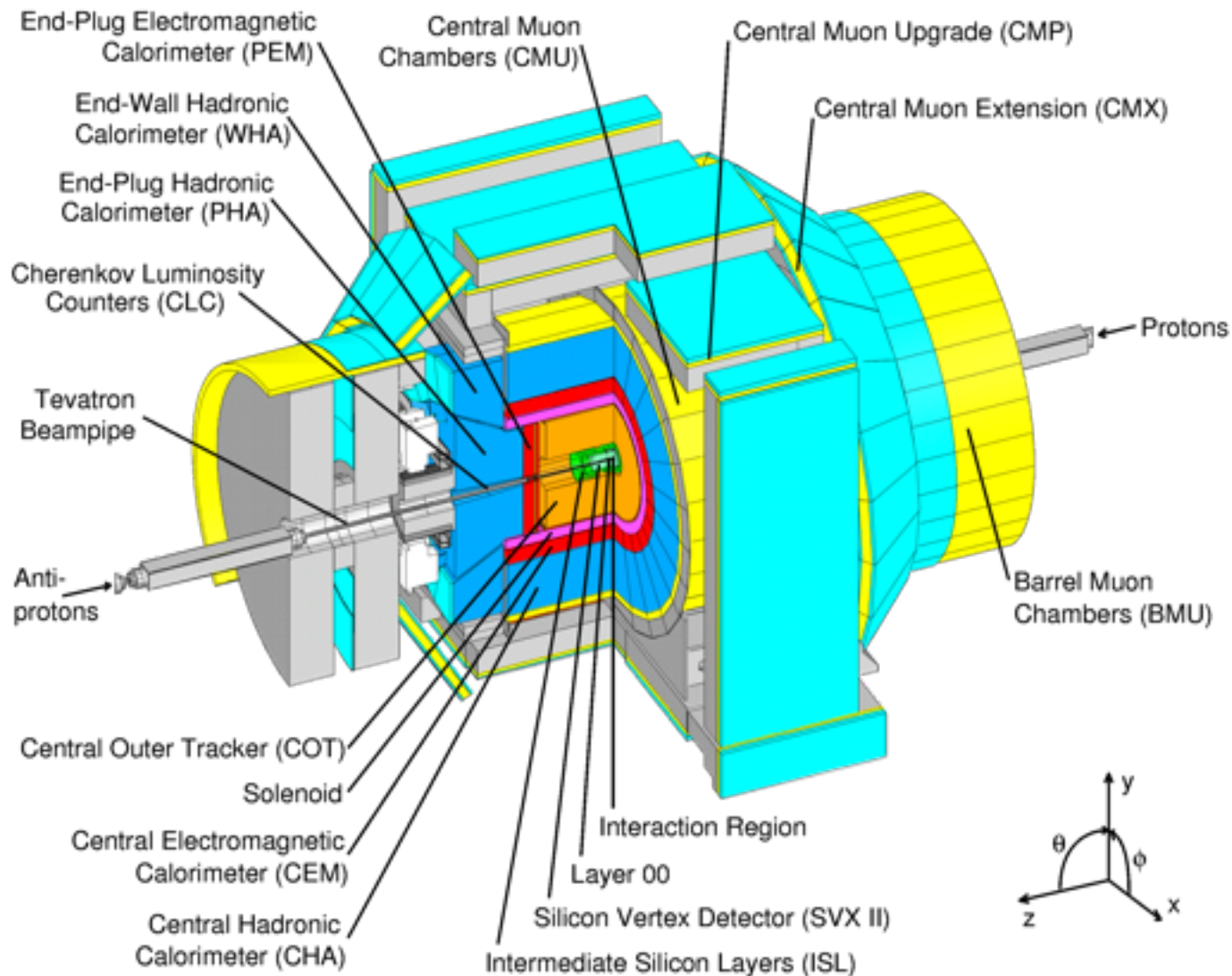
Proton-antiproton collider operating at a collision energy of 1.8 TeV in 1992-96 (Run I) and 1.96 TeV in 2001-11 (Run II)

World's highest-energy collider until 2010

- ✓ Located at Fermilab near Chicago
- ✓ 1 km radius
- ✓ **1976**: Construction started
- ✓ **1985**: Commissioning
- ✓ **1987**: CDF Run 0
- ✓ Continuous upgrades over 25 years of operations



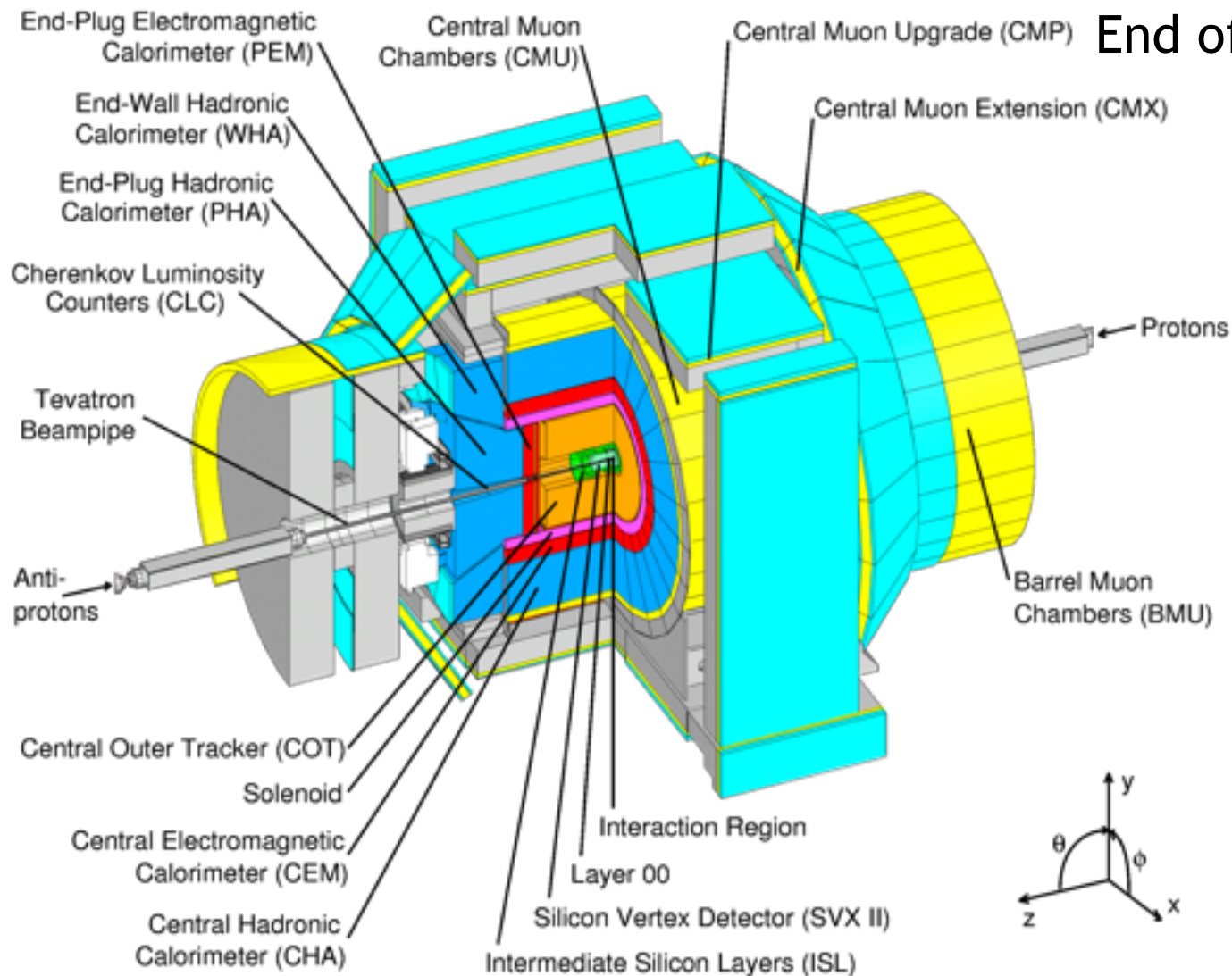
The Collider Detector at Fermilab (CDF)



The Collider Detector at Fermilab (CDF)

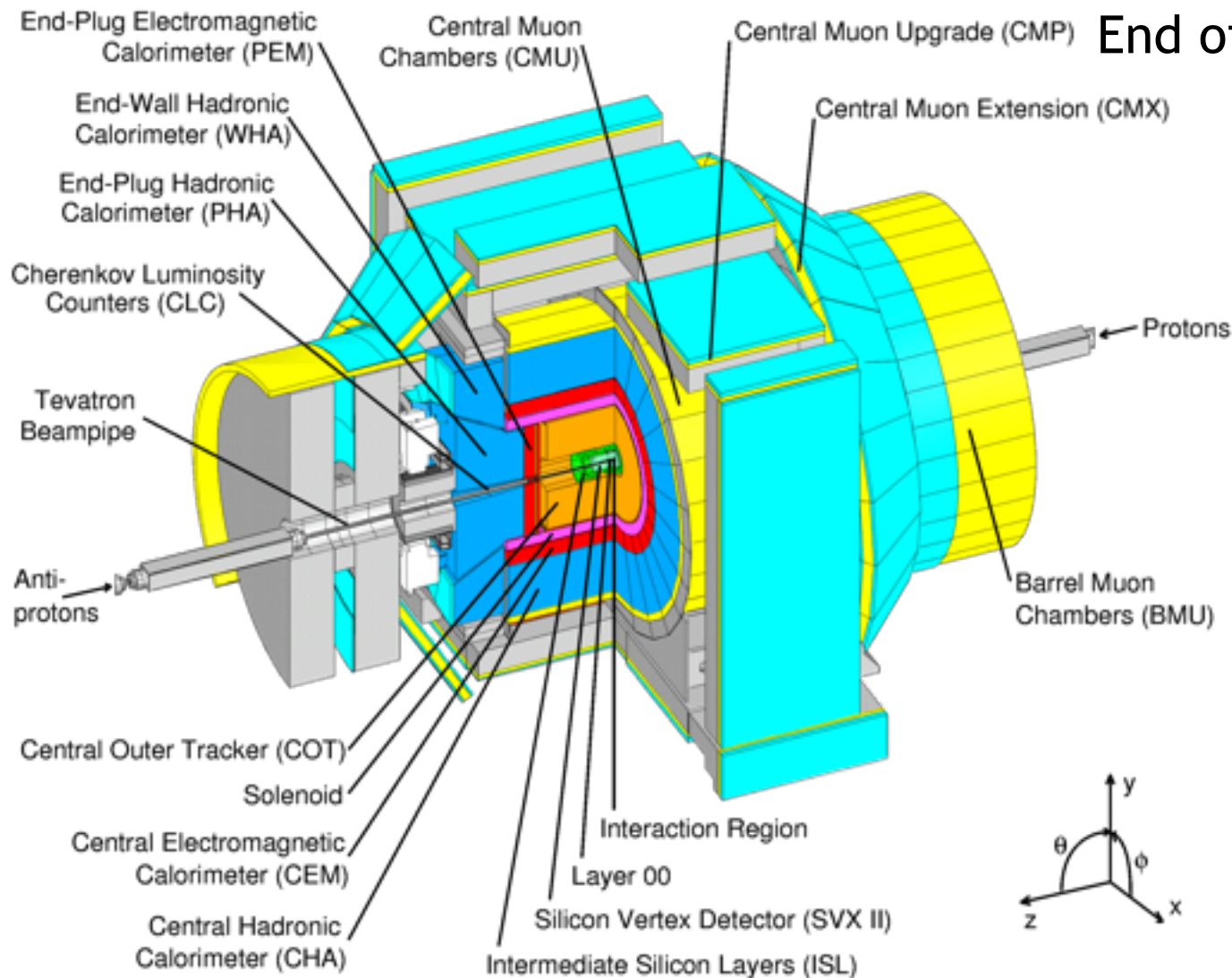
First CDF $p\bar{p}$ event: 1985

End of operations: 2011



The Collider Detector at Fermilab (CDF)

First CDF $p\bar{p}$ event: 1985
End of operations: 2011



Lepton
coverage:

$$|\eta| < 2.0 \text{ (e)}$$

$$|\eta| < 1.5 \text{ (\mu)}$$

Jets to $|\eta| < 2.8$

b-tagging with
 $|\eta| < 1.5$

Selection criteria of top pair candidate events

	0-tag	1-tagL	1-tagT	2-tagL	2-tagT
Lepton p_T (GeV)	> 20	> 20	> 20	> 20	> 20
Lepton η	< 1	< 1	< 1	< 1	< 1
1st 3 jets E_T (GeV)	> 20	> 20	> 20	> 20	> 20
1st 3 jets η	< 2	< 2	< 2	< 2	< 2
4th jet E_T (GeV)	> 20	> 12	> 20	> 12	> 20
4th jet η	< 2	< 2.4	< 2	< 2.4	< 2
Extra jets	$E_T < 20$	Any L $\geq 1 T$	Any L	Any L $\geq 1 T$	Any L
b-tags ($\eta < 1.5$)	0	1	1	> 1	> 1
Missing E_T (GeV)	> 20	> 20	> 20	> 20	> 20
$\Delta\phi(E_T, \text{jet})$ (rad)	> 0.5	> 0.5	> 0.5	Any	Any

Estimated sample composition at 9 fb^{-1} luminosity

	0-tag	1-tagL	1-tagT	2-tagL	2-tagT	All
<i>W + h.f.</i>	697	357	161	34	21	1269
<i>W + l.f.</i>	1581	171	77	3	2	1834
<i>Z + jets</i>	169	25	14	2	1	212
<i>Dibosons</i>	166	31	18	3	2	220
<i>Single top</i>	14	17	8	7	5	50
<i>QCD</i>	623	120	60	1	6	811
<i>Background</i>	3251	720	338	49	37	4395
<i>Signal</i>	960	999	1086	331	425	3801
<i>Total</i>	4211	1719	1424	380	462	8196
<i>S/B</i>	0.3	1.4	3.2	6.8	10.6	0.9
<i>Observed</i>	4474	1711	1434	365	375	8359

Definition of the likelihood

$$N(m_t) = \int_{z_1 z_2} |M|^2 \frac{f(z_1) f(z_2)}{z_1 z_2} dz_1 dz_2 d\Phi(\vec{y})$$

w_{ij} = permutation weight depending on # of b-tags

$$L_i^s(m_t, \Delta_{JES}) = \frac{1}{N(m_t)} \frac{1}{A(m_t, \Delta_{JES})} \sum_{j=1}^{24} w_{ij} P(\vec{x}_i | m_t, \Delta_{JES}) \quad A = \frac{N_{sel}(m_t, \Delta_{JES})}{N_{tot}(m_t)}$$

$$P(\vec{x} | m_t, \Delta_{JES}) = \int T(\vec{x} | \vec{y}, \Delta_{JES}) \left| M_{2p \rightarrow lv_1+4p}^{t\bar{t}}(m_t, \vec{y}) \right|^2 \times \frac{f(z_1, Q^2) f(z_2, Q^2)}{z_1 z_2} \Big|_{Q=2m_t} dz_1 dz_2 d\Phi(\vec{y})$$

$$\int T(\vec{x} | \vec{y}, \Delta_{JES}) d^3 x = \varepsilon(\vec{y})$$

$$d\Phi(\vec{y}) = \prod_{k=1}^6 \frac{d^3 y_k}{(2\pi)^3 2E_k}$$

Integration elements

➤ $M_{2p \rightarrow lv_l+4p}^{t\bar{t}}$: Kleiss-Stirling LO ME, including qq, gg, & spin correlations, R. Kleiss and W. J. Stirling, Z. Phys. **40**, 419 (1988)

➤ $M_{2p \rightarrow lv_l+4p}^W$: Madgraph5 W + 4 partons ME, J. Alwall *et al.*, JHEP07, 079 (2014)

➤ f : CTEQ5L, H. L. Lai *et al.*, Eur. Phys. J. C **12**, 375 (2000)

➤ $T = F_1 \left(\frac{p_T^j}{p_T^p}, p_T^p, \eta_p, m \right) F_2 \left(\Delta\eta_{j-p}, \Delta\phi_{j-p}, p_T^p, \eta_p, m \right)$: From MC, separately for b & light jets

➤ Integration variables: $2 \times \{m_t^2, m_W^2\}, \log(p_1 / p_2)_{W \rightarrow j_1 j_2}, \vec{p}_T^{t\bar{t}}, 4 \times \{\eta, \phi, m\}_p$

➤ Quasi-MC integration, F. J. Hickernell and L. A. JimenezRugama, arXiv:1410.8615: 18 variables integrated using importance sampling, m_W^2 integrated with a grid-based procedure because of phase space singularities when $\partial m_W^2 / \partial p_z^y = 0$

Mu2e backup

Significance

➤ Backgrounds

Category	Background process	Estimated yield (events)
Intrinsic	Muon decay-in-orbit (DIO)	0.199 ± 0.092
	Muon radiative capture (RMC)	$0.000^{+0.004}_{-0.000}$
Late arriving	Pion radiative capture (RPC)	0.023 ± 0.006
	Muon decay-in-flight (μ -DIF)	< 0.003
	Pion decay-in-flight (π -DIF)	0.001 ± 0.001
	Beam electrons	0.003 ± 0.001
Miscellaneous	Antiproton induced	0.047 ± 0.024
	Cosmic ray induced	0.096 ± 0.020
Total		0.37 ± 0.10

Significance

➤ Backgrounds

Category	Background process	Estimated yield (events)
Intrinsic	Muon decay-in-orbit (DIO)	0.199 ± 0.092
	Muon radiative capture (RMC)	$0.000^{+0.004}_{-0.000}$
Late arriving	Pion radiative capture (RPC)	0.023 ± 0.006
	Muon decay-in-flight (μ -DIF)	< 0.003
	Pion decay-in-flight (π -DIF)	0.001 ± 0.001
	Beam electrons	0.003 ± 0.001
Miscellaneous	Antiproton induced	0.047 ± 0.024
	Cosmic ray induced	0.096 ± 0.020
Total		0.37 ± 0.10

➤ Bottom line:

- ✓ Single event sensitivity: $R_{\mu e} = 2.8 \times 10^{-17}$
- ✓ 90% C.L. (if no signal) : $R_{\mu e} < 7 \times 10^{-17}$
- ✓ Typical SUSY Signal: ~ 50 events or more

Significance

➤ Backgrounds

Category	Background process	Estimated yield (events)
Intrinsic	Muon decay-in-orbit (DIO)	0.199 ± 0.092
	Muon radiative capture (RMC)	$0.000^{+0.004}_{-0.000}$
Late arriving	Pion radiative capture (RPC)	0.023 ± 0.006
	Muon decay-in-flight (μ -DIF)	< 0.003
	Pion decay-in-flight (π -DIF)	0.001 ± 0.001
	Beam electrons	0.003 ± 0.001
Miscellaneous	Antiproton induced	0.047 ± 0.024
	Cosmic ray induced	0.096 ± 0.020
Total		0.37 ± 0.10

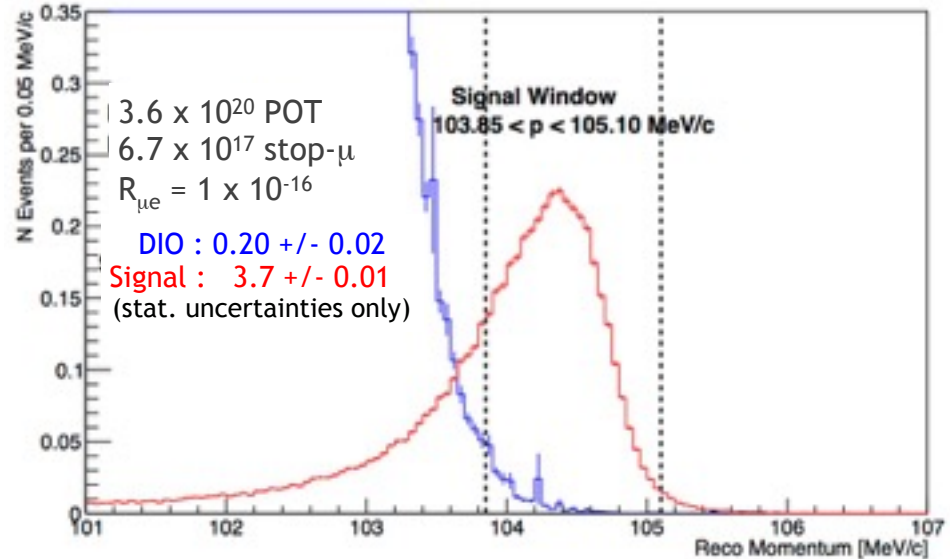
➤ Bottom line:

- ✓ Single event sensitivity: $R_{\mu e} = 2.8 \times 10^{-17}$
- ✓ 90% C.L. (if no signal) : $R_{\mu e} < 7 \times 10^{-17}$
- ✓ Typical SUSY Signal: ~ 50 events or more

4 orders of
magnitude
improvement!

Sensitivity

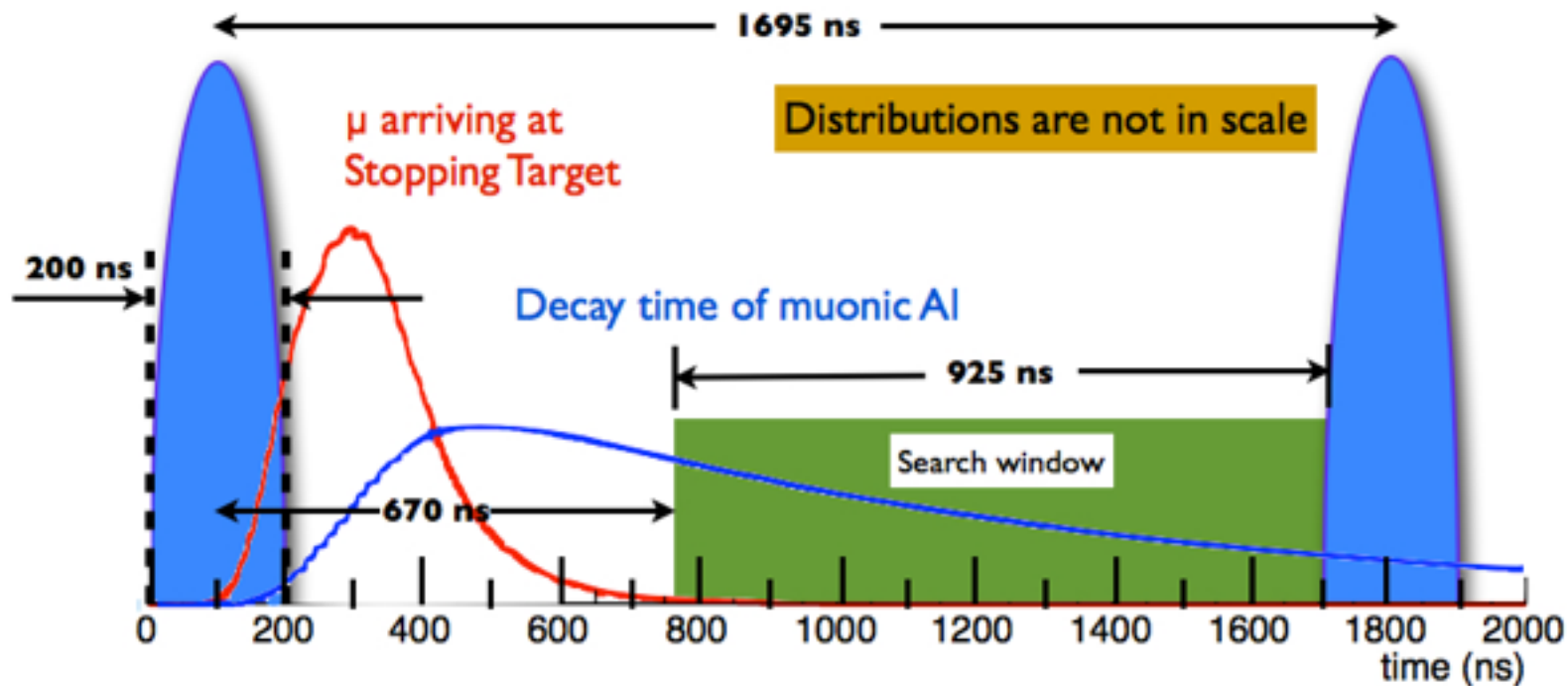
- Cuts chosen to maximize significance
- 3.6×10^{20} protons on target
 - ✓ 3 years nominal running



Parameter	Value
Running time @ 2×10^7 s/yr.	3 years
Protons on target per year	1.2×10^{20}
μ^- stops in stopping target per proton on target	0.0016
μ^- capture probability	0.609
Fraction of muon captures in live time window	0.51
Electron Trigger, Selection, and Fitting Efficiency in Live Window	0.10

Single Event Sensitivity: $R_{\mu e} = 3 \times 10^{-17}$

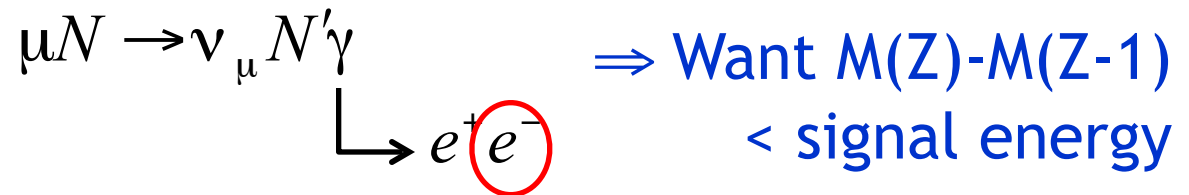
Event time structure



- μ^- are accompanied by e^- , π^- , ...
- Extinction system makes prompt background ~equal to all other backgrounds
 - ✓ 1 out of time proton per 10^{10} in time protons
- Lifetime of muonic Al: 864 ns

Mu2e (MELC) experimental technique

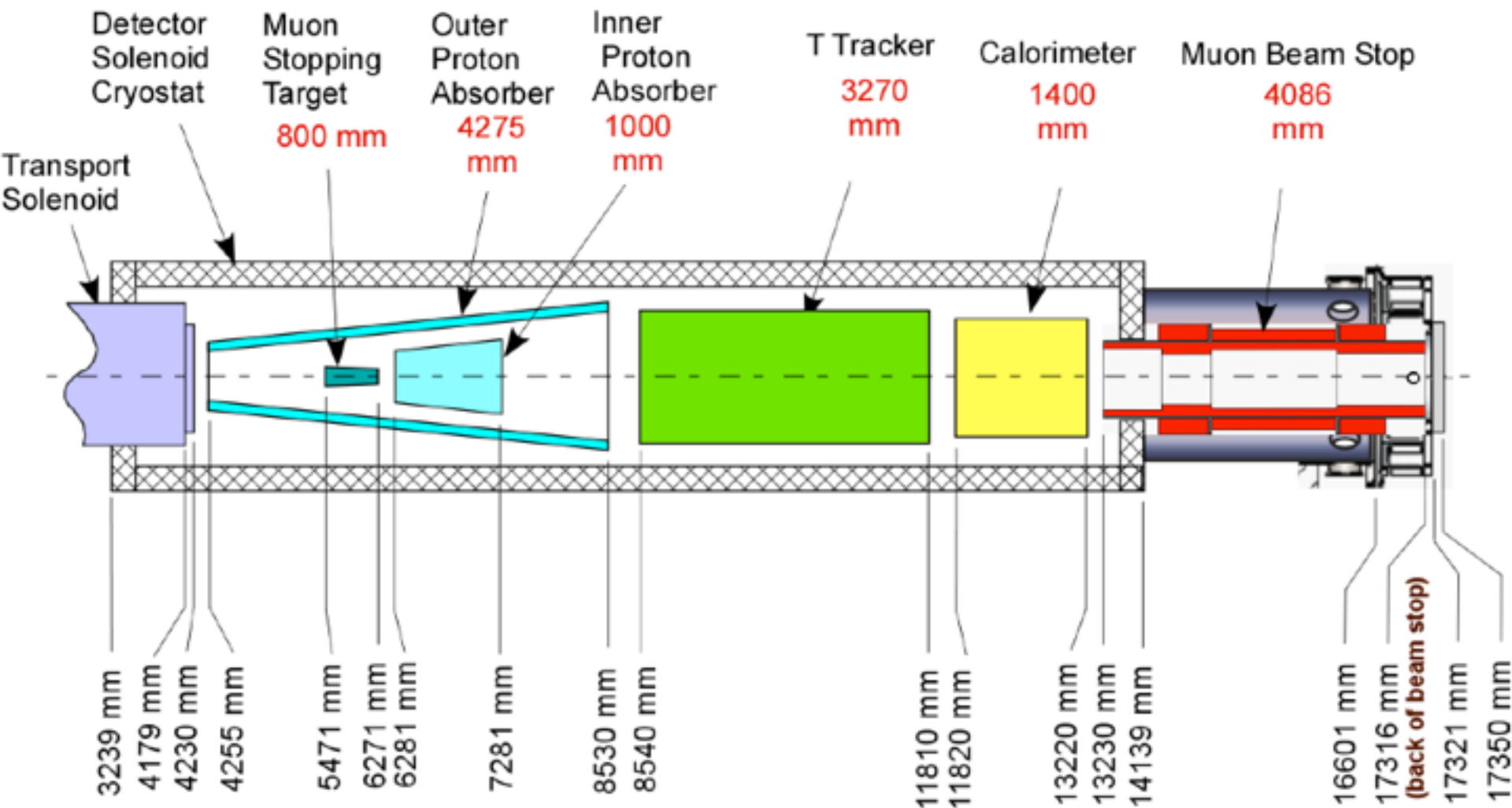
- Determining the Z dependence is very important, but
- Lifetime is *shorter* for high-Z
 - ✓ Decreases useful live window
- Also, need to avoid background from radiative muon capture



\Rightarrow Aluminum is nominal choice for Mu2e

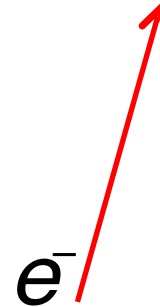
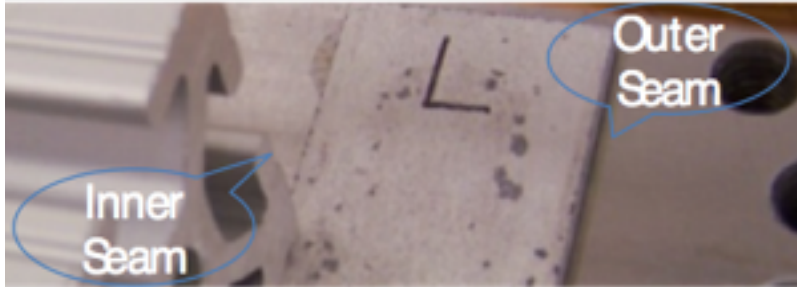
Nucleus	$R_{\mu e}(Z) / R_{\mu e}(Al)$	Bound lifetime	Atomic Bind. Energy(1s)	Conversion Electron Energy	Prob decay >700 ns
Al(13,27)	1.0	.88 μ s	0.47 MeV	104.97 MeV	0.45
Ti(22,~48)	1.7	.328 μ s	1.36 MeV	104.18 MeV	0.16
Au(79,~197)	~0.8-1.5	.0726 μ s	10.08 MeV	95.56 MeV	negligible

Target and detector complex



Particle tracking technology

- To achieve the required resolution, must keep mass as low as possible to minimize scattering
- We've chosen transverse planes of "straw chambers" (21,600 straws)



- Track ionizes gas in tube
- Charge drifts to sense wire at center
- Drift time gives precision position

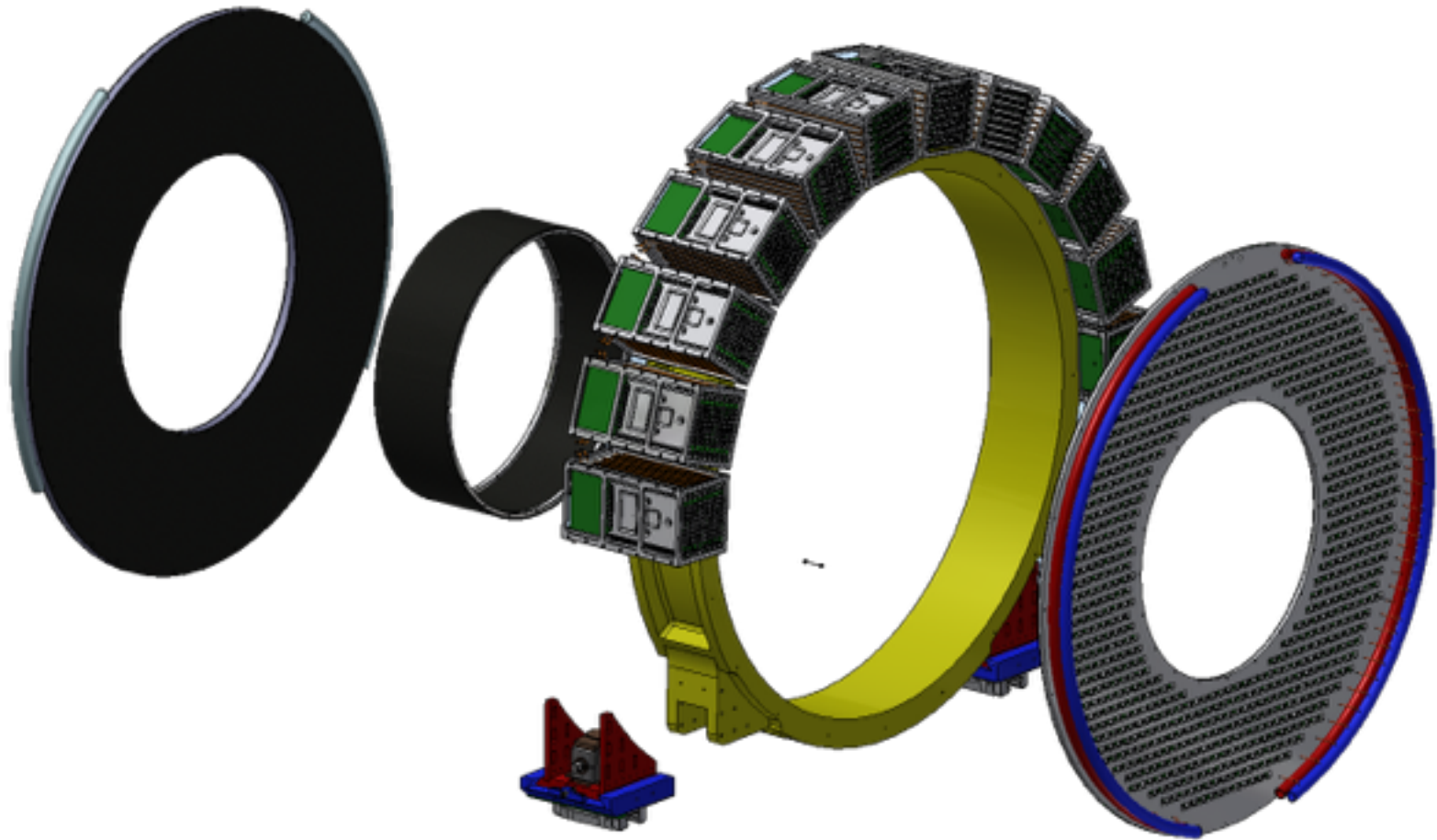
➤ Advantages

- ✓ Established technology
- ✓ Broken wires isolated
- ✓ Modular: support, gas, and electronic connections at the ends, outside of tracking volume

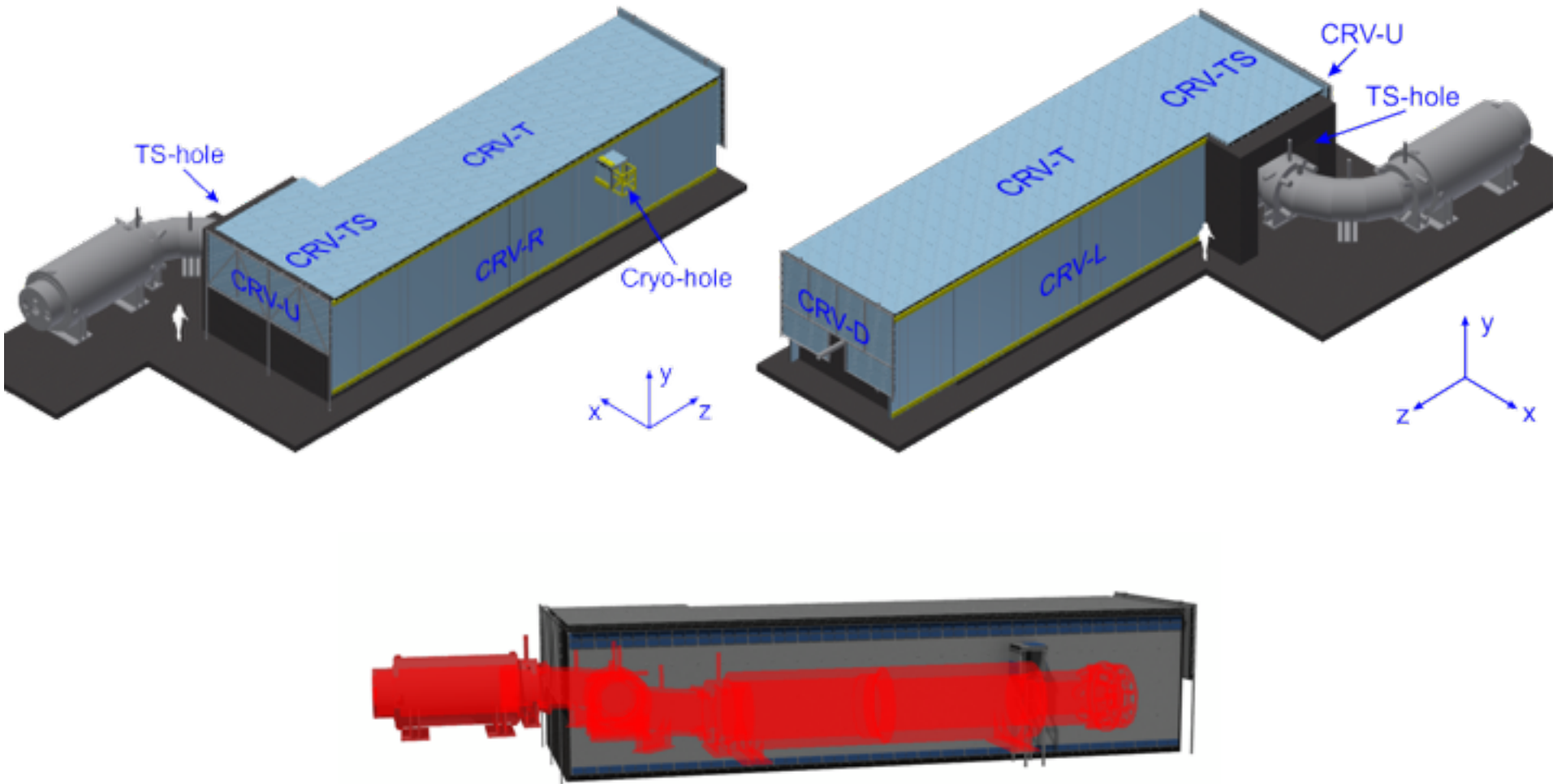
➤ Challenges

- ◇ Our specified wall thickness (15 μm) has never been done
- ◇ Operating in a vacuum may be problematic

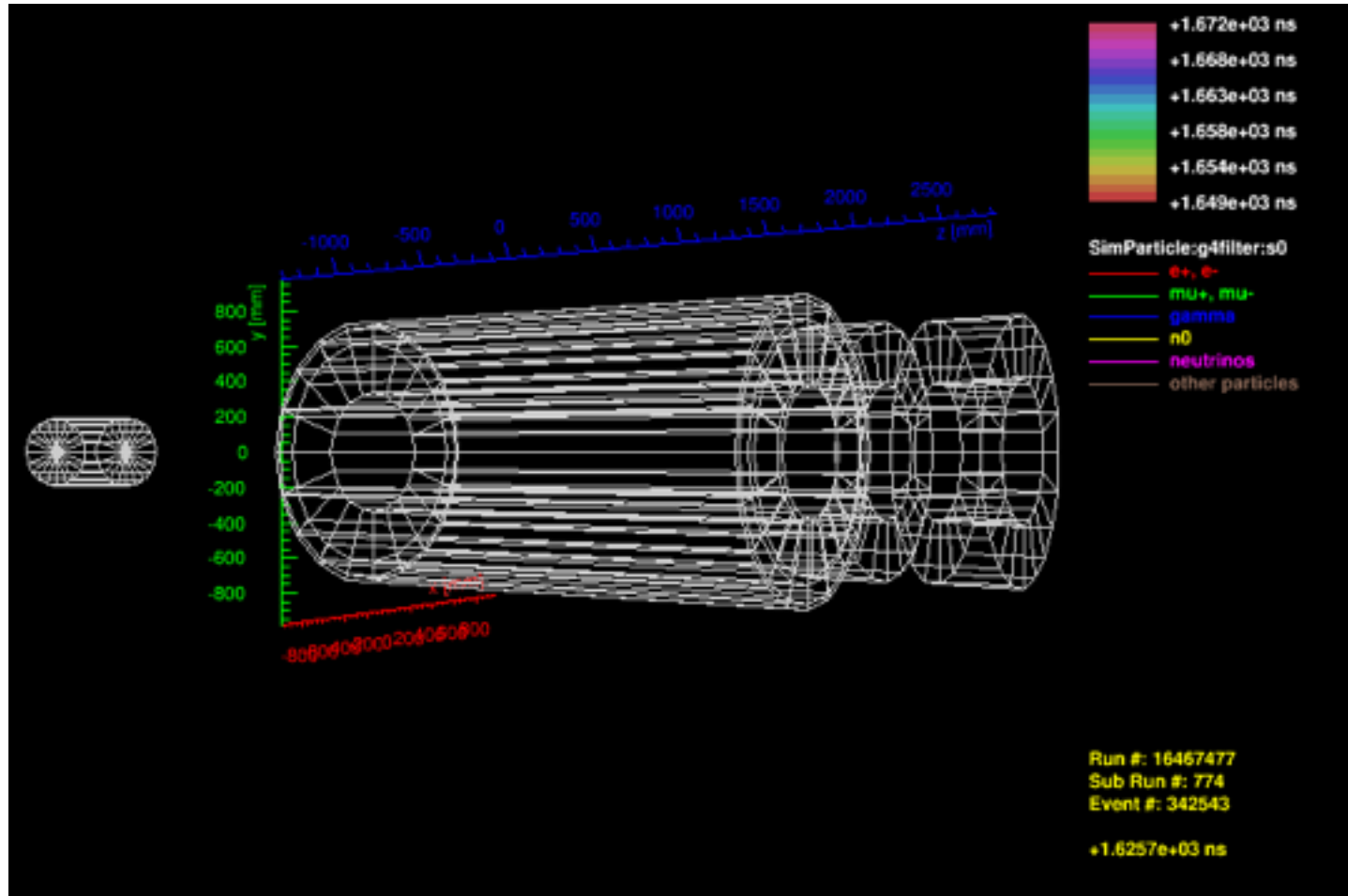
A calorimeter annulus: exploded view



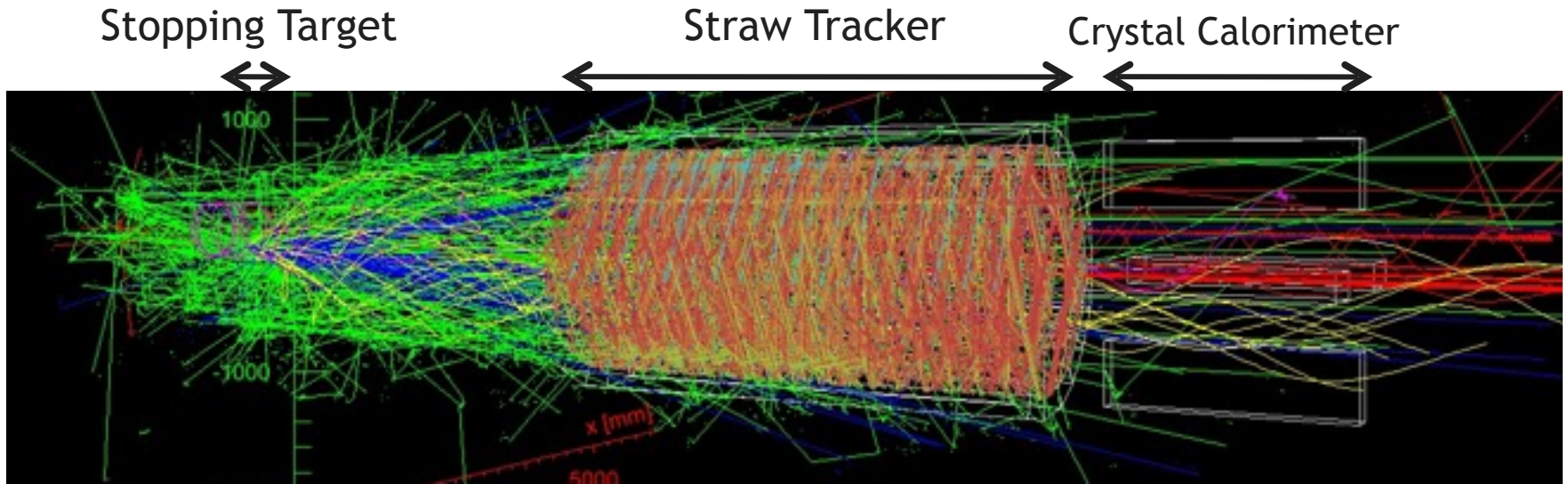
Layout of the CRV



A 105 MeV cosmic-induced electron



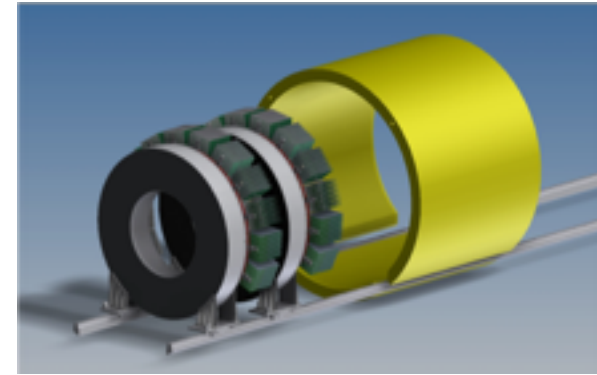
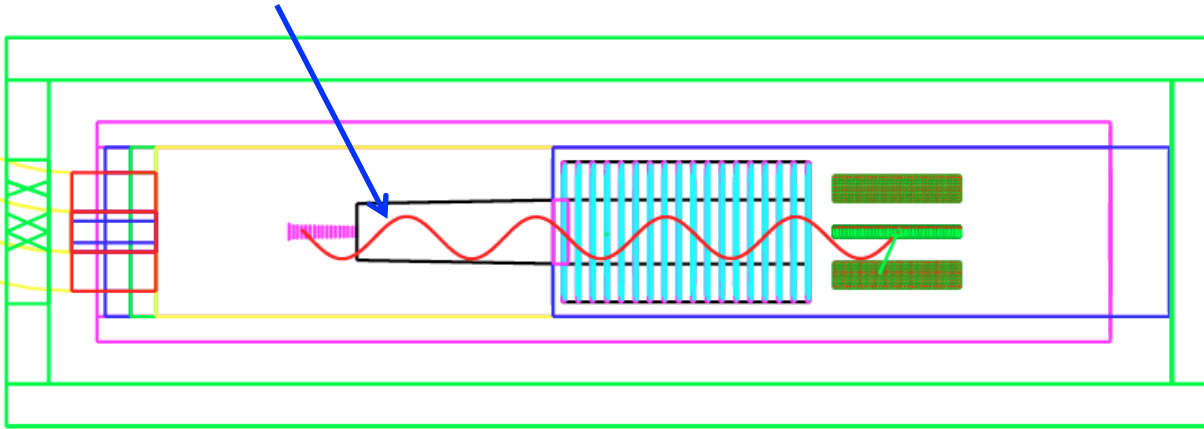
Background overlays



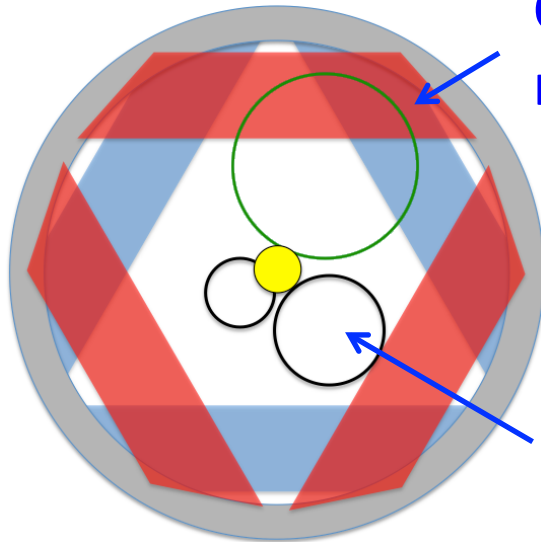
We simulate a full $\sim 1\mu\text{s}$, including all the background overlays from the beam flash, μ -capture products, neutrons, etc. and we properly account for contributions from previous bunches

Particle detector

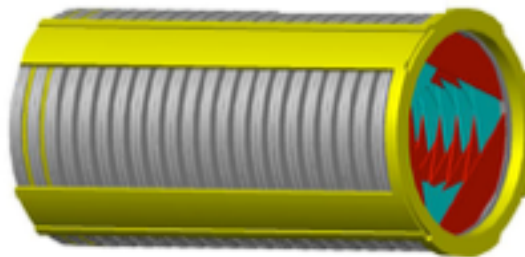
Helical trajectory



Conversions hit multiple planes.

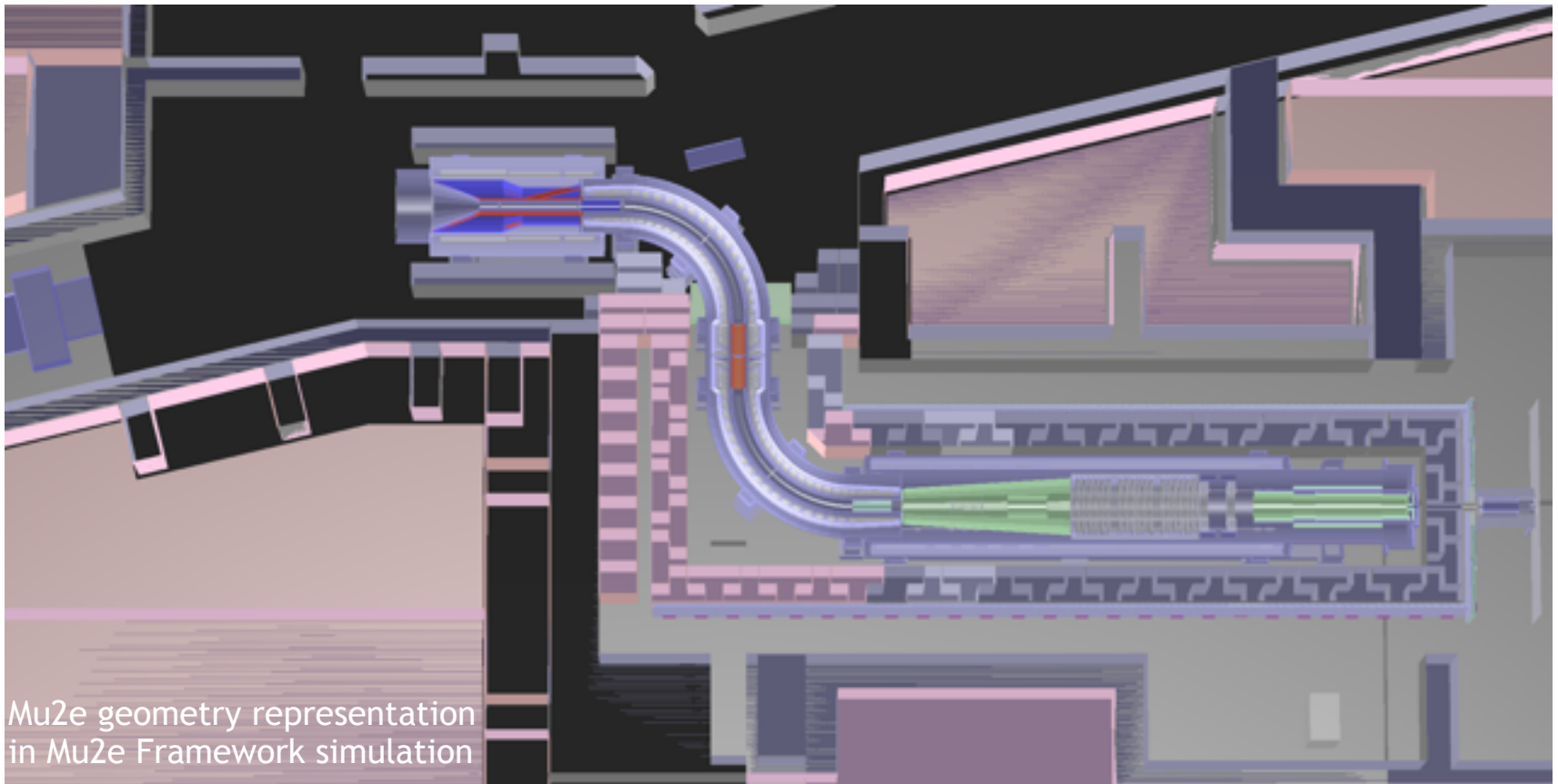


Crystal calorimeter to tag electrons



Most decays ($p_T < 53 \text{ MeV}/c$) go down the middle (vacuum)

Simulation model



Detailed model of solenoids, targets, detectors, supports, shielding, building, soil and back-fill materials, etc.

Mu2e experimental hall under construction

